FIG. 5. Frequencies of Gag$_{241-249}$-specific CD8$^+$ T cells detected by Gag$_{241-249}$-Mamu-A*90120-5 tetramers after a SIV challenge. (A) Frequencies of Gag$_{241-249}$-Mamu-A*90120-5 tetramer$^+$ cells within CD8$^+$ T cells in group III animals before a challenge (week 0) or at week 2 after a challenge. A representative dot plot gated on CD3$^+$ lymphocytes for determining tetramer$^+$ CD8$^+$ T cells (x axis, CD8; y axis, tetramer) in macaque R07-008 is shown in the lower panel. (B) Tetramer$^+$ CD28$^-$ cell frequencies in CD8$^+$ T cells in group III animals at weeks 0 and 2. Data on tetramer$^+$ CD95$^+$ CD28$^-$ CD8$^+$ T-cell frequencies at week 0 are unavailable. (C) Tetramer$^+$ CD95$^+$ CD28$^-$ CD8$^+$ T-cell frequencies in naive controls (groups I and II) and group III animals at week 2. The bar indicates the geometric mean of each group. The frequencies in group III were significantly higher than those in naive controls (P = 0.0001 by unpaired t test). Samples from macaques R06-019 in group I and R07-007 in group III were unavailable for this analysis.

tion of viral loads in the acute phase. These results suggest that this vaccination approach altered the dominance pattern of CD8$^+$ T-cell responses and resulted in dominant induction of effective Gag$_{241-249}$-specific CD8$^+$ T-cell responses in the

acute phase after a SIV challenge, facilitating a reduction in peak viral loads. Selection of vaccine epitopes for induction of CD8$^+$ T-cell responses might be important for viral control because the antiviral efficacy of CD8$^+$ T cells could be affected by MHC-I-restricted target epitopes (10, 19, 25, 35).

Gag$_{241-249}$-specific CD8$^+$ T-cell induction by prophylactic vaccination resulted in higher frequencies of these T-cell responses during the acute phase after the SIV challenge. The induction of Gag$_{241-249}$-specific effector memory CD8$^+$ T cells was especially marked. We did not examine polyfunctionality, but analyses of a cytolytic marker, CD107a, indicated higher frequencies of Gag$_{241-249}$-specific cytolytic CD8$^+$ T-cell responses, implying that these T cells originating from vaccine-induced memory may have higher cytolytic activity in the acute phase. These results suggest that group III animals with Gag$_{241-249}$-specific memory CD8$^+$ T cells showed induction of a high magnitude of Gag$_{241-249}$-specific CD8$^+$ T cells with effector function after a SIV challenge, resulting in reduction of viral loads in the acute phase.

In this study, some 90-120-Ia-positive unvaccinated macaques showed lower viral loads. However, in our previous studies with Burmese rhesus macaques (reference 15 and unpublished data), all unvaccinated 90-120-Ia-negative animals failed to contain a SIVmac239 challenge and animals, including vaccinees, that failed to control SIVmac239 replication developed AIDS in 1 to 4 years; even R-90-120 descendants possessing the MHC-I haplotype 90-120-Ib but not 90-120-Ia (both 90-120-Ia and 90-120-Ib are derived from breeder R-90-120) showed high viral loads. Additionally, 90-120-Ia-positive animals failed to control the replication of SIVmac239 carrying CTL escape mutations (16). Thus, a SIVmac239 challenge of Burmese rhesus macaques mostly results in persistent viremia and progression to AIDS but some 90-120-Ia-positive animals may show lower viral loads due to 90-120-Ia-associated SIV-specific CTL responses. However, a previously reported 90-120-Ia-positive unvaccinated macaque, R02-007, developed AIDS around 3 years after a SIVmac239 challenge. Furthermore, two of the 90-120-Ia-positive vaccinees that controlled a SIVmac239 challenge but showed reappearance of viremia
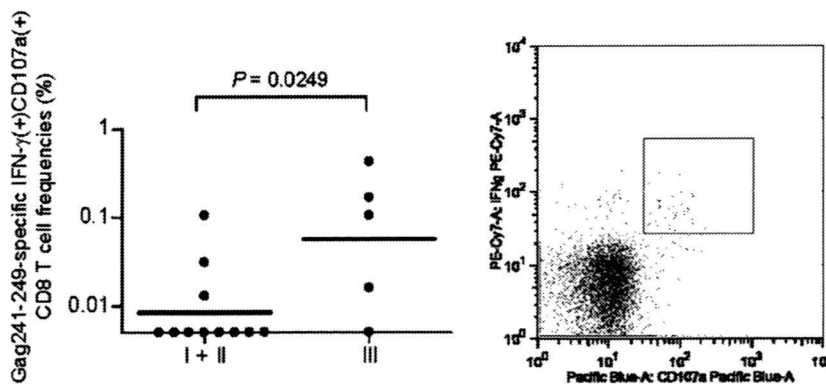
FIG. 6. Gag$_{241-249}$-specific cytolytic CD8$^+$ T-cell frequencies at week 2 after a challenge. PBMCs were cultured in the absence or the presence of the Gag$_{241-249}$ peptide for unstimulated controls or Gag$_{241-249}$-specific stimulation, and the frequencies of CD8$^+$ T cells exhibiting Gag$_{241-249}$-specific induction of both IFN-γ and CD107a in the total CD8$^+$ T cells were examined. The bar indicates the geometric mean of each group. The frequencies in group III were significantly higher than those in naive controls (P = 0.0249 by unpaired t test). The right panel is a representative dot plot showing the CD107a (x axis) and IFN-γ (y axis) responses in CD8$^+$ T cells in macaque R07-008 after Gag$_{241-249}$-specific stimulation. Samples from macaques R06-019 in group I and R07-007 in group III were unavailable for this analysis.

around 1 year later developed AIDS (15). Thus, it is inferred that the majority of *90-120-Ia*-positive unvaccinated macaques develop AIDS after a SIVmac239 challenge. Several MHC-I alleles are known to be associated with lower viral loads in HIV and SIV infections, and potent CTLs directed against these MHC-I-restricted epitopes have been implicated in the suppression of viral replication (7, 8, 9, 10, 13, 18, 22, 31, 33, 48). The $Gag_{241-249}$-specific CTL may also be naturally potent (10, 16), but the impact of memory induction of even these potent CTLs on viral control has not yet been determined. Thus, this is the first study documenting the benefit of single-epitope-specific memory $CD8^+$ T-cell induction by prophylactic vaccination for HIV/SIV control. Further analysis with a vaccine expressing a single helper epitope, as well as a CTL epitope, would contribute to evaluation of the impact of HIV/SIV-specific $CD4^+$ T-cell memory induction on HIV/SIV replication.

Because $CCR5^+$ memory $CD4^+$ T cells, especially HIV-specific $CD4^+$ T cells, are themselves targets of this virus, whether virus-specific $CD4^+$ T-cell induction by prophylactic vaccination can result in effective virus-specific $CD4^+$ T-cell responses postinfection and contribute to HIV control remains unclear. On the other hand, it has been unknown whether HIV-specific memory $CD8^+$ T cells induced by vaccination without HIV-specific $CD4^+$ T-cell help can elicit effective responses after virus exposure. In the present study, the $pGag_{236-250}$-EGFP/F($-$)SeV-$Gag_{236-250}$-EGFP vaccination elicited $Gag_{241-249}$-specific $CD8^+$ T-cell responses without SIV-specific $CD4^+$ T-cell help but possibly with EGFP-specific or SeV-specific $CD4^+$ T-cell help; i.e., SeV-EGFP-specific $CD4^+$ T cells would confer cognate help for $Gag_{241-249}$-specific $CD8^+$ T-cell induction. The $Gag_{241-249}$-specific memory $CD8^+$ T cells induced by prophylactic vaccination without SIV-specific $CD4^+$ T-cell help but with non-SIV-specific $CD4^+$ T-cell responses responded efficiently to a SIV challenge, showing dominant $Gag_{241-249}$-specific $CD8^+$ T-cell responses resulting in SIV control; infection-induced SIV-specific $CD4^+$ T-cell responses may be involved in $Gag_{241-249}$-specific $CD8^+$ T-cell induction postinfection. Therefore, this study documents that prophylactic vaccination eliciting virus-specific $CD8^+$ T-cell memory even without virus-specific $CD4^+$ T-cell responses (but with cognate non-virus-specific $CD4^+$ T-cell responses) can facilitate SIV control after a challenge.

Taken together, the present study demonstrates that induction of single-epitope-specific $CD8^+$ T-cell memory without virus-specific $CD4^+$ T-cell help by prophylactic vaccination can result in dominant potent $CD8^+$ T-cell responses and control of SIV replication after a challenge. These results imply possible HIV control by prophylactic vaccination eliciting virus-specific $CD8^+$ T-cell memory with non-virus-specific $CD4^+$ T-cell help and provide valuable insights into AIDS vaccine development.

ACKNOWLEDGMENTS

REFERENCES

1. **Anonymous.** 2007. Cold shower for AIDS vaccines. Nat. Med. **13:**1389–1390.
2. **Argüello, J. R., A. M. Little, A. L. Pay, D. Gallardo, I. Rojas, S. G. Marsh, J. M. Goldman, and J. A. Madrigal.** 1998. Mutation detection and typing of polymorphic loci through double-strand conformation analysis. Nat. Genet. **18:**192–194.
3. **Borrow, P., H. Lewicki, B. H. Hahn, G. M. Shaw, and M. B. Oldstone.** 1994. Virus-specific $CD8^+$ cytotoxic T-lymphocyte activity associated with control of viremia in primary human immunodeficiency virus type 1 infection. J. Virol. **68:**6103–6110.
4. **Brander, C., and B. D. Walker.** 1999. T lymphocyte responses in HIV-1 infection: implication for vaccine development. Curr. Opin. Immunol. **11:**451–459.
5. **Douek, D. C., J. M. Brenchley, M. R. Betts, D. R. Ambrozak, B. J. Hill, Y. Okamoto, J. P. Casazza, J. Kuruppu, K. Kunstman, S. Wolinsky, Z. Grossman, M. Dybul, A. Oxenius, D. A. Price, M. Connors, and R. A. Koup.** 2002. HIV preferentially infects HIV-specific $CD4^+$ T cells. Nature **417:**95–98.
6. **Feinberg, M. B., and J. P. Moore.** 2002. AIDS vaccine models: challenging challenge viruses. Nat. Med. **8:**207–210.
7. **Friedrich, T. C., E. J. Dodds, L. J. Yant, L. Vojnov, R. Rudersdorf, C. Cullen, D. T. Evans, R. C. Desrosiers, B. R. Mothe, J. Sidney, A. Sette, K. Kunstman, S. Wolinsky, M. Piatak, J. Lifson, A. L. Hughes, N. Wilson, D. H. O'Connor, and D. I. Watkins.** 2004. Reversion of CTL escape-variant immunodeficiency viruses in vivo. Nat. Med. **10:**275–281.
8. **Goulder, P. J., M. Bunce, P. Krausa, K. McIntyre, S. Crowley, B. Morgan, A. Edwards, P. Giangrande, R. E. Phillips, and A. J. McMichael.** 1996. Novel, cross-restricted, conserved, and immunodominant cytotoxic T lymphocyte epitopes in slow progressors in HIV type 1 infection. AIDS Res. Hum. Retrovir. **12:**1691–1698.
9. **Goulder, P. J., and D. I. Watkins.** 2004. HIV and SIV CTL escape: implications for vaccine design. Nat. Rev. Immunol. **4:**630–640.
10. **Goulder, P. J. R., and D. I. Watkins.** 2008. Impact of MHC class I diversity on immune control of immunodeficiency virus replication. Nat. Rev. Immunol. **8:**619–630.
11. **Janssen, E. M., E. E. Lemmens, T. Wolfe, U. Christen, M. G. von Herrath, and S. P. Schoenberger.** 2003. $CD4^+$ T cells are required for secondary expansion and memory in $CD8^+$ T lymphocytes. Nature **421:**852–856.
12. **Jin, X., D. E. Bauer, S. E. Tuttleton, S. Lewin, A. Gettie, J. Blanchard, C. E. Irwin, J. T. Safrit, J. Mittler, L. Weinberger, L. G. Kostrikis, L. Zhang, A. S. Perelson, and D. D. Ho.** 1999. Dramatic rise in plasma viremia after $CD8^+$ T cell depletion in simian immunodeficiency virus-infected macaques. J. Exp. Med. **189:**991–998.
13. **Kaslow, R. A., M. Carrington, R. Apple, L. Park, A. Muñoz, A. J. Saah, J. J. Goedert, C. Winkler, S. J. O'Brien, C. Rinaldo, R. Detels, W. Blattner, J. Phair, H. Erlich, and D. L. Mann.** 1996. Influence of combinations of human major histocompatibility complex genes on the course of HIV-1 infection. Nat. Med. **2:**405–411.
14. **Kawada, M., H. Igarashi, A. Takeda, T. Tsukamoto, H. Yamamoto, S. Dohki, M. Takiguchi, and T. Matano.** 2006. Involvement of multiple epitope-specific cytotoxic T-lymphocyte responses in vaccine-based control of simian immunodeficiency virus replication in rhesus macaques. J. Virol. **80:**1949–1958.
15. **Kawada, M., T. Tsukamoto, H. Yamamoto, A. Takeda, H. Igarashi, D. I. Watkins, and T. Matano.** 2007. Long-term control of simian immunodeficiency virus replication with central memory $CD4^+$ T-cell preservation after nonsterile protection by a cytotoxic T-lymphocyte-based vaccine. J. Virol. **81:**5202–5211.
16. **Kawada, M., T. Tsukamoto, H. Yamamoto, N. Iwamoto, K. Kurihara, A. Takeda, C. Moriya, H. Takeuchi, H. Akari, and T. Matano.** 2008. Gag-specific cytotoxic T lymphocyte-based control of primary simian immunodeficiency virus replication in a vaccine trial. J. Virol. **82:**10199–10206.
17. **Kestler, H. W., III, D. J. Ringler, K. Mori, D. L. Panicali, P. K. Sehgal, M. D. Daniel, and R. C. Desrosiers.** 1991. Importance of the nef gene for maintenance of high virus loads and for development of AIDS. Cell **65:**651–662.
18. **Kiepiela, P., A. J. Leslie, I. Honeyborne, D. Ramduth, C. Thobakgale, S. Chetty, P. Rathnavalu, C. Moore, K. J. Pfafferott, L. Hilton, P. Zimbwa, S. Moore, T. Allen, C. Brander, M. M. Addo, M. Altfeld, I. James, S. Mallal, B. Bunce, L. D. Barber, J. Szinger, C. Day, P. Klenerman, J. Mullins, B. Korber, H. M. Coovadia, B. D. Walker, and P. J. Goulder.** 2004. Dominant influence of HLA-B in mediating the potential co-evolution of HIV and HLA. Nature **432:**769–775.
19. **Kiepiela, P., K. Ngumbela, C. Thobakgale, D. Ramduth, I. Honeyborne, E. Moodley, S. Reddy, C. de Pierres, Z. Mncube, N. Mkhwanazi, K. Bishop, M. van der Stok, K. Nair, N. Khan, H. Crawford, R. Payne, A. Leslie, J. Prado,**

A. Prendergast, J. Frater, N. McCarthy, C. Brander, G. H. Learn, D. Nickle, C. Rousseau, H. Coovadia, J. I. Mullins, D. Heckerman, B. D. Walker, and P. Goulder. 2007. CD8^{+} T-cell responses to different HIV proteins have discordant associations with viral load. Nat. Med. 13:46–53.

20. Koup, R. A., J. T. Safrit, Y. Cao, C. A. Andrews, G. McLeod, W. Borkowsky, C. Farthing, and D. D. Ho. 1994. Temporal association of cellular immune responses with the initial control of viremia in primary human immunodeficiency virus type 1 syndrome. J. Virol. 68:4650–4655.

21. Lamoreaux, L., M. Roederer, and R. Koup. 2006. Intracellular cytokine optimization and standard operating procedure. Nat. Protoc. 1:1507–1516.

22. Leslie, A. J., K. J. Pfafferott, P. Chetty, R. Draenert, M. M. Addo, M. Feeney, Y. Tang, E. C. Holmes, T. Allen, J. G. Prado, M. Altfeld, C. Brander, C. Dixon, D. Ramduth, P. Jeena, S. A. Thomas, A. St. John, T. A. Roach, B. Kupfer, G. Luzzi, A. Edwards, G. Taylor, H. Lyall, G. Tudor-Williams, V. Novelli, J. Martinez-Picado, P. Kiepiela, B. D. Walker, and P. J. Goulder. 2004. HIV evolution: CTL escape mutation and reversion after transmission. Nat. Med. 10:282–289.

23. Letvin, N. L., J. R. Mascola, Y. Sun, D. A. Gorgone, A. P. Buzby, L. Xu, Z. Y. Yang, B. Chakrabarti, S. S. Rao, J. E. Schmitz, D. C. Montefiori, B. R. Barker, F. L. Bookstein, and G. J. Nabel. 2006. Preserved CD4^{+} central memory T cells and survival in vaccinated SIV-challenged monkeys. Science 312:1530–1533.

24. Li, H. O., Y. F. Zhu, M. Asakawa, H. Kuma, T. Hirata, Y. Ueda, Y. S. Lee, M. Fukumura, A. Iida, A. Kato, Y. Nagai, and M. Hasegawa. 2000. A cytoplasmic RNA vector derived from nontransmissible Sendai virus with efficient gene transfer and expression. J. Virol. 74:6564–6569.

25. Loffredo, J. T., A. T. Bean, D. R. Beal, E. J. León, G. E. May, S. M. Piaskowski, J. R. Furlott, J. Reed, S. K. Musani, E. G. Rakasz, T. C. Friedrich, N. A. Wilson, D. B. Allison, and D. I. Watkins. 2008. Patterns of CD8^{+} immunodominance may influence the ability of Mamu-B*08-positive macaques to naturally control simian immunodeficiency virus SIVmac239 replication. J. Virol. 82:1723–1738.

26. Matano, T., M. Kano, H. Nakamura, A. Takeda, and Y. Nagai. 2001. Rapid appearance of secondary immune responses and protection from acute CD4 depletion after a highly pathogenic immunodeficiency virus challenge in macaques vaccinated with a DNA-prime/Sendai viral vector-boost regimen. J. Virol. 75:11891–11896.

27. Matano, T., M. Kobayashi, H. Igarashi, A. Takeda, H. Nakamura, M. Kano, C. Sugimoto, K. Mori, A. Iida, T. Hirata, M. Hasegawa, T. Yuasa, M. Miyazawa, Y. Takahashi, M. Yasunami, A. Kimura, D. H. O'Connor, D. I. Watkins, and Y. Nagai. 2004. Cytotoxic T lymphocyte-based control of simian immunodeficiency virus replication in a preclinical AIDS vaccine trial. J. Exp. Med. 199:1709–1718.

28. Matano, T., R. Shibata, C. Siemon, M. Connors, H. C. Lane, and M. A. Martin. 1998. Administration of an anti-CD8 monoclonal antibody interferes with the clearance of chimeric simian/human immunodeficiency virus during primary infections of rhesus macaques. J. Virol. 72:164–169.

29. Mattapallil, J. J., N. L. Letvin, and M. Roederer. 2004. T-cell dynamics during acute SIV infection. AIDS 18:13–23.

30. McMichael, A. J., and T. Hanke. 2003. HIV vaccines 1983-2003. Nat. Med. 9:874–880.

31. Migueles, S. A., M. S. Sabbaghian, W. L. Shupert, M. P. Bettinotti, F. M. Marincola, L. Martino, C. W. Hallahan, S. M. Selig, D. Schwartz, J. Sullivan, and M. Connors. 2000. HLA B*5701 is highly associated with restriction of virus replication in a subgroup of HIV-infected long term nonprogressors. Proc. Natl. Acad. Sci. USA 97:2709–2714.

32. National Institute of Infectious Diseases. 2007. Guides for animal experiments performed at National Institute of Infectious Diseases. National Institute of Infectious Diseases, Tokyo, Japan. (In Japanese.)

33. O'Connor, D. H., B. R. Mothe, J. T. Weinfurter, S. Fuenger, W. M. Rehrauer, P. Jing, R. R. Rudersdorf, M. E. Liebl, K. Krebs, J. Vasquez, E. Dodds, J. Loffredo, S. Martin, A. B. McDermott, T. M. Allen, C. Wang, G. G. Doxiadis, D. C. Montefiori, A. Hughes, D. R. Burton, D. B. Allison, S. M. Wolinsky, R. Bontrop, L. J. Picker, and D. I. Watkins. 2003. Major histocompatibility complex class I alleles associated with slow simian immunodeficiency virus

disease progression bind epitopes recognized by dominant acute-phase cytotoxic-T-lymphocyte responses. J. Virol. 77:9029–9040.

34. Pitcher, C. J., S. I. Hagen, J. M. Walker, R. Lum, B. L. Mitchell, V. C. Maino, M. K. Axthelm, and L. J. Picker. 2002. Development and homeostasis of T cell memory in rhesus macaques. J. Immunol. 168:29–43.

35. Reynolds, M. R., A. M. Weiler, K. L. Weisgrau, S. M. Piaskowski, J. R. Furlott, J. T. Weinfurter, M. Kaizu, T. Soma, E. J. León, C. MacNair, D. P. Leaman, M. B. Zwick, E. Gostick, S. K. Musani, D. A. Price, T. C. Friedrich, E. G. Rakasz, N. A. Wilson, A. B. McDermott, R. Boyle, D. B. Allison, D. R. Burton, W. C. Koff, and D. I. Watkins. 2008. Macaques vaccinated with live-attenuated SIV control replication of heterologous virus. J. Exp. Med. 205:2537–2550.

36. Rosenberg, E. S., J. M. Billingsley, A. M. Caliendo, S. L. Boswell, P. E. Sax, S. A. Kalams, and B. D. Walker. 1997. Vigorous HIV-1-specific CD4^{+} T cell responses associated with control of viremia. Science 278:1447–1450.

37. Schmitz, J. E., M. J. Kuroda, S. Santra, V. G. Sasseville, M. A. Simon, M. A. Lifton, P. Racz, K. Tenner-Racz, M. Dalesandro, B. J. Scallon, J. Ghrayeb, M. A. Forman, D. C. Montefiori, E. P. Rieber, N. L. Letvin, and K. A. Reimann. 1999. Control of viremia in simian immunodeficiency virus infection by CD8^{+} lymphocytes. Science 283:857–860.

38. Seder, R. A., P. A. Darrah, and M. Roederer. 2008. T-cell quality in memory and protection: implications for vaccine design. Nat. Rev. Immunol. 8:247–258.

39. Shaffer, J. P. 1986. Modified sequentially rejective multiple test procedures. J. Am. Stat. Assoc. 81:826–831.

40. Shedlock, D. J., and H. Shen. 2003. Requirement for CD4 T cell help in generating functional CD8 T cell memory. Science 300:337–339.

41. Shibata, R., F. Maldarelli, C. Siemon, T. Matano, M. Parta, G. Miller, T. Fredrickson, and M. A. Martin. 1997. Infection and pathogenicity of chimeric simian-human immunodeficiency viruses in macaques: determinants of high virus loads and CD4 cell killing. J. Infect. Dis. 176:362–373.

42. Staprans, S. I., A. P. Barry, G. Silvestri, J. T. Safrit, N. Kozyr, B. Sumpter, H. Nguyen, H. McClure, D. Montefiori, J. I. Cohen, and M. B. Feinberg. 2004. Enhanced SIV replication and accelerated progression to AIDS in macaques primed to mount a CD4 T cell response to the SIV envelope protein. Proc. Natl. Acad. Sci. USA 101:13026–13031.

43. Sun, J. C., and M. J. Bevan. 2003. Defective CD8 T cell memory following acute infection without CD4 T cell help. Science 300:339–342.

44. Tanaka-Takahashi, Y., M. Yasunami, T. Naruse, K. Hinohara, T. Matano, K. Mori, M. Miysazawa, M. Honda, Y. Yasutomi, Y. Nagai, and A. Kimura. 2007. Reference strand-mediated conformation analysis (RSCA)-based typing of multiple alleles in the rhesus macaque MHC class I Mamu-A and Mamu-B loci. Electrophoresis 28:918–924.

45. Tsukamoto, T., S. Dohki, T. Ueno, M. Kawada, A. Takeda, M. Yasunami, T. Naruse, A. Kimura, M. Takiguchi, and T. Matano. 2008. Determination of a major histocompatibility complex class I restricting simian immunodeficiency virus Gag241-249 epitope. AIDS 22:993–994.

46. Vaccari, M., J. Mattapallil, K. Song, W. P. Tsai, A. Hryniewicz, D. Venzon, M. Zanetti, K. A. Reimann, M. Roederer, and G. Franchini. 2008. Reduced protection from simian immunodeficiency virus SIVmac251 infection afforded by memory CD8^{+} T cells induced by vaccination during CD4^{+} T-cell deficiency. J. Virol. 82:9629–9638.

47. Wilson, N. A., J. Reed, G. S. Napoe, S. Piaskowski, A. Szymanski, J. Furlott, E. J. Gonzalez, L. J. Yant, N. J. Maness, G. E. May, T. Soma, M. R. Reynolds, E. Rakasz, R. Rudersdorf, A. B. McDermott, D. H. O'Connor, T. C. Friedrich, D. B. Allison, A. Patki, L. J. Picker, D. R. Burton, J. Lin, L. Huang, D. Patel, G. Heindecker, J. Fan, M. Citron, M. Horton, F. Wang, X. Liang, J. W. Shiver, D. R. Casimiro, and D. I. Watkins. 2006. Vaccine-induced cellular immune responses reduce plasma viral concentrations after repeated low-dose challenge with pathogenic simian immunodeficiency virus SIVmac239. J. Virol. 80:5875–5885.

48. Yant, L. J., T. C. Friedrich, R. C. Johnson, G. E. May, N. J. Maness, A. M. Enz, J. D. Lifson, D. H. O'Connor, M. Carrington, and D. I. Watkins. 2006. The high-frequency major histocompatibility complex class I allele Mamu-B*17 is associated with control of simian immunodeficiency virus SIVmac239 replication. J. Virol. 80:5074–5077.

1
2
3
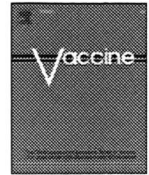
T cell-based functional cDNA library screening identified SEC14-like 1a carboxy-terminal domain as a negative regulator of human immunodeficiency virus replication

4 Emiko Urano [a,b], Reiko Ichikawa [a], Yuko Morikawa [b], Takeshi Yoshida [c], Yoshio Koyanagi [c], Jun Komano [a,*]

6 [a] National Institute of Infectious Diseases, 1-23-1 Toyama, Shinjuku-ku, Tokyo 162-8640, Japan
7 [b] Graduate School of Infection Control Sciences, Kitasato University, Shirokane 5-9-1, Minato-ku, Tokyo 108-8641, Japan
8 [c] Laboratory of Viral Pathogenesis, Institute for Virus Research, Kyoto University, Kyoto 606-8507, Japan

ARTICLE INFO

ABSTRACT

Genome-wide screening of host factors that regulate HIV-1 replication has been attempted using numerous experimental approaches. However, there has been limited success using T cell-based cDNA library screening to identify genes that regulate HIV-1 replication. We have established a genetic screening strategy using the human T cell line MT-4 and a replication-competent HIV-1. With this system, we identified the C-terminal domain (CTD) of SEC14-like 1a (SEC14L1a) as a novel inhibitor of HIV-1 replication. Our T cell-based cDNA screening system provides an alternative tool for identifying novel regulators of HIV-1 replication.

© 2009 Published by Elsevier Ltd.

1. Introduction

The molecular interaction between HIV-1 and the host is not fully understood. A systematic genome-wide approach provides the critical information for the completion of the HIV-1-host interactome. Many experimental genome-wide screening systems have been established to identify the cellular genes required for HIV-1 replication (Table 1, [1–8]). More than a hundred genes have been identified as being cellular factors that regulate HIV-1 replication. However, different screening systems do not identify the same set of genes, and many systems yielded non-overlapping candidates. These discrepancies are assumed to be due to differences in the experimental approaches, such as the virus, the cell line, or the genetic materials used.

For viruses, the wild-type HIV-1 [1,3–6] or a replication-incompetent HIV-1 pseudotyped with vesicular stomatitis virus (VSV)-G is used [2,7,8]. The VSV-G-pseudotyped "HIV-1-based vector" has been used to identify factors associated with the viral entry processes. However, in reality, it covers the events from post-membrane fusion to translation. One of the potential caveats in the use of the VSV-G-pseudotyped vector is that it enters cells via the VSV-G-restricted route, which is fundamentally different from the HIV-1 Env-mediated entry pathway [9–12]. The replication-competent HIV-1 should be ideal to cover the entire viral replication cycle; however, this may raise biosafety concerns.

For cells, non-T cells, such as a genetically engineered HeLa cells that ectopically express luciferase or beta-galactosidase (TZM-bl cells), are often used, since they are efficiently transduced with genetic materials [2,5–8]. Not many studies employ a T cell-based system, partly because genetic materials are not efficiently transduced into T cells [1,3,4]. To identify HIV-1 replication regulatory factors, it is preferable to perform the functional analysis in the natural targets of HIV-1 including T cells. The gene expression profile of non-T cells is apparently different from that of T cells as exemplified by the absence of T cell specific markers on non-T cells such as CD4. It is possible that a candidate gene isolated in the non-T cell-based system might not be expressed in T cells. It is impossible to identify T cell-specific factors in the non-T cell-based screening using the siRNA library or in the screening using cDNA libraries derived from non-T cells. Also, the effect or functions of some genes may not be identical in distinct cell types. The potential risk of a non-T cell-based assay is that we may falsely score a gene as a regulator of HIV-1 replication, although many genes have been discovered using non-T cell-based screening systems including the viral receptors. Ideally, the primary CD4-positive T cells, dendritic cells, macrophages, or NK/T cells should be used.

---

* Corresponding author at: AIDS Research Center, National Institute of Infectious Diseases, 1-23-1 Toyama, Shinjuku, Tokyo 162-8640, Japan. Tel.: +81 3 5285 1111; fax: +81 3 5285 5037.
E-mail address: ajkomano@nih.go.jp (J. Komano).

2　　　　　　　　　　　　　　　　　　　E. Urano et al. / Vaccine xxx (2009) xxx–xxx

Table 1
Summary of genome-wide screening strategies to identify regulatory factors of HIV-1 replication.

Genetic material	Transduction approach	Cell line	Replication competency of HIV-1	Reference
cDNA library	Retroviral, stable	TE671	Incompetent	[2,8]
siRNA library	Transfection, transient	HeLa or 293T	Competent or incompetent	[5,6,7]
cDNA library	Lenti- or retroviral, stable	MT-4	Competent	[1,3,4]

Given technical limitations, this is currently unrealistic for genetic screening experiments.

As for the genetic material, cDNA libraries are often used [1–4,8]. Recent studies utilized siRNA libraries [5–7]. The cDNA approach is advantageous for providing genetic diversity. Expression of the full-length open reading frame of a gene can upregulate the function of the gene, whereas cDNA fragments can function in a diverse fashion. The gene silencing approach downregulates gene expression; however, the silencing efficiency of a gene varies in different cell types and at different time points in the assay (reviewed in [13]). As mentioned above, the gene silencing approach is unable to score the contribution of genes that are not expressed in the cells used in the assay.

The screening can be performed in cells that are either transiently [5–7] or stably [1–4,8] transduced with genetic materials. In the transient transfection assays, it is possible that the dysregulation of a gene function can damage the physiology of the cells. In such a case, the inhibition of HIV-1 replication can be observed, but may not be a direct inhibitory effect of the gene of interest. Such a risk can be minimized by using cells stably transduced with the genetic materials.

We conducted a phenotype cDNA screen using a T cell line-based assay to identify cellular genes that render cells resistant to HIV-1 replication [3]. The advantage of our functional screening system is that cDNA libraries are stably transduced into cells, and that a replication-competent HIV-1 and a human T cell line MT-4 are used. With this system, we have successfully identified the SEC14-like 1a (SEC14L1a) C-terminal domain (CTD) as an inhibitor of HIV-1 replication that targets the late phase of the viral life cycle.

2. Materials and methods

2.1. Cells, transfection, cDNA selection

Cells were maintained in RPMI 1640 medium (Sigma, St. Louis, MA) supplemented with 10% fetal bovine serum (Japan Bioserum, Tokyo, Japan), 100 U/ml penicillin, and 100 μg/ml streptomycin (Invitrogen, Tokyo, Japan). Cells were incubated at 37 °C in a humidified 5% CO_2 atmosphere. Cells were transfected with Lipofectamine 2000 according to the manufacturer's protocol (Invitrogen). The method of selecting human cDNAs that confer resistance to HIV-1 has been described previously in detail [3].

2.2. Plasmids

The SEC14L1a CTD1 was amplified from MT-4 polyA RNA by reverse transcriptase PCR (RT-PCR) using the primers 5'-GCACCGG-TCTCGAGCCACCATGGACTACAAAGACGATGACGACCCTGCGTGCGC-CGCCAGCAGC-3' and 5'-CCAATTGCTACCTGGAGATCATGGAGCTG-3'. The SEC14L1a CTD2 was amplified by PCR from human lymph node cDNA library (Takara, Otsu, Japan) using the primers 5'-GCAC-CGGTCTCGAGCCACCATGGACTACAAAGACGATGACGACTGCGAAG-TGCCAGAGGGTGGAC-3' and 5'-CCAATTGCTACCTGGAGATCAT-GGAGCTG-3'. Full length (FL) SEC14L1a was amplified by PCR from a plasmid containing the SEC14L1a open reading frame (ORF, CS0DL004YN18, Invitrogen), using the primers 5'-GCA-CCGGTCTCGAGCCACCATGGACTACAAAGACGATGACGACGTGCAG-AAATACCAGTCCCCAG-3' and 5'-CCAATTGCTACCTGGAGATCATGG-

AGCTG-3'. The AgeI-MfeI fragments of the PCR products were cloned into the XmaI-MfeI sites of the pEGFP-C3 plasmid (Clontech, Palo Alto, CA), generating pEGFP-SEC14L1a-CTD1, -CTD2, and -FL. The XhoI-MfeI fragments from the resulting plasmids were cloned into the corresponding restriction sites of the pCMMP KRAB vector, creating pCMMP GFP-SEC14L1a-CTD1, -CTD2, and -FL. The HIV-1 *tat* was amplified by PCR using the primers 5'-AACCGGTCTCGAGCCACCATGGAGCCAGTAGATCCTAGAC-3' and 5'-GGATCCTCAGTCGTCATCGTCTTTGTAGTCTTCCTTCGGGCCTGTCGG-GTC-3'. A Tat expression vector pCMMP Tat was constructed by cloning the AgeI-BamHI fragment of the PCR product into the corresponding restriction sites of the pCMMP KRAB vector. The HIV-1 *Env* and GFP expression vectors (pIIIex and pCMMP GFP, respectively) are described previously [3,12,14]. To construct the pCMMP GFP-FLAG (GFPf), pCMMP CXCR4 d-10 [15] was digested with AgeI and XhoI to remove CXCR4 d-10 ORF and self-ligated after blunting with T4 DNA polymerase. The HIV-1 *gag-pol*, *tat*, and *rev* expressing plasmid pCMVR8.91 was a generous gift from Dr. Trono's group [16].

2.3. Western blotting

Western blotting was performed according to techniques described previously [17]. The following reagents were used: anti-FLAG (rabbit polyconal, 600-401-383, Rockland, Gilbertsville, PA), anti-p24 (183-H12-5C, NIH AIDS Research and Reference Reagent Program), anti-gp120 (vA-20 and vT-21 antibodies, Santa Cruz Biotech, Santa Cruz, CA), biotinylated anti-goat antibody (GE Healthcare Bio-Sciences, Piscataway, NJ), horseradish peroxidase-conjugated streptoavidin (GE Healthcare Bio-Sciences), and EnVision+ system (Dako, Glostrup, Denmark). Signals were visualized with an LAS3000 imager (Fujifilm, Tokyo, Japan) and quantified by Multi Gauge ver 3.0 software (Fujifilm).

2.4. Confocal microscopy

293T cells transiently transfected with expression vectors for SEC14L1a derivatives were grown on glass plates, fixed in 4% formaldehyde in phosphate buffer saline (PBS) for 5 min at 24 h post-transfection, stained with Hoechst 33258 (Sigma), mounted (Vectorshield, Vector Laboratories, Burlingame, CA), and imaged using a confocal microscope META 510 (Carl Zeiss, Tokyo, Japan). For MT-4 cells, live cells were incubated with Hoechst 33258 and imaged unfixed. Image brightness and contrast were processed by META510 software (Carl Zeiss).

2.5. Immunoprecipitation

Cells expressing FLAG-tagged proteins were harvested and washed twice with PBS and then lysed in the lysis buffer (50 mM Tris-HCl, pH 8.0, 0.5% IGEPAL CA630, protease inhibitor cocktail from Sigma) on ice for 30 min. The soluble fraction was obtained by centrifugation at 15,000 rpm for 30 min at 4 °C, and was incubated with 20 μl of Red-Anti-FLAG M2 Affinity Gel (Sigma) with gentle mixing overnight at 4 °C. After washing the agarose beads for five times with the lysis buffer, the bound complexes were eluted with the FLAG peptide, and analyzed by Western blotting.

2.6. Flow cytometry

Cells were labeled with PE-Cy5-conjugated anti-CD4 antibody or PE-conjugated anti-CXCR4 antibody (Beckton Dickinson, San Jose, Calif.) for 30 min at 4 C. Cells were washed once with PBS supplemented with 1% FBS and analyzed by FACS Aria (Beckton Dickinson). The GFP-positive cells were sorted using FACS Aria.

2.7. Monitoring HIV-1 replication

For HIV-1 infection, 1×10^5 cells were incubated at the room temperature with the HIV-1$_{HXB2}$-containing culture supernatant, which had approximately 1.0 ng of p24^{CA}, for approximately 30 min. The culture supernatants were collected at 4 d post-infection and subjected to ELISA to measure the p24^{CA} antigen, using a Retro TEK p24 Antigen ELISA Kit according to the manufacturer's protocol (Zepto Metrix, Buffalo, NY). The signals were measured with an ELx808 microplate photometer (BIO-TEK®, Winooski, VT).

2.8. PCR analysis

The cellular DNA and RNA were extracted from cells infected with VSV-G-pseudotyped HIV-1 vector produced by using pNL-Luc plasmid, as described previously [17]. The Alu-LTR PCR and RT-PCR were performed as described previously [3,17] using the following primers: for the first Alu-LTR PCR reaction, 5'-AACTAGGGAACCCACTGCTTAAG-3' and 5'-TGCTGGGATTACAGGC-GTGAG-3'; and for the second Alu-LTR PCR reaction, 5'-AACT-AGGGAACCCACTGCTTAAG-3' and 5'-CTGCTAGAGATTTTCCACA-CTGAC-3'. For amplification of HIV-1 mRNA, 5'-ATGGAGCCAGTAG-ATCCTAGAC-3' and 5'-CTATTCCTTCGGGCCTGTCGGG-3' primers were used. For the control, we amplified beta-globin and cyclophilin A using the following primers: beta-globin, 5'-TATTGGTCT-CCTTAAACCTGTCTTG-3' and 5'-CTGACACAACTGTGTTCACTAGC-3'; and cyclophilin A, 5'-CACCGCCACCATGGTCAACCCCACCGTGTTCT-TCGAC-3' and 5'-CCCGGGCCTCGAGCTTTCGAGTTGTCCACAGTCA-GCAATGG-3'. The amplicons were separated in a 2% agarose gel, stained with ethidium bromide, and imaged with a Typhoon scanner (GE Healthcare Bio-Sciences).

2.9. Collection of virus-like particle

Tissue culture supernatants containing virus-like particles (VLP) were passed through nitrocellulose filters (0.45 μm, Millipore, Tokyo, Japan) and the virions were collected by centrifugation (Optima™ TL, TLA 100.3 rotor, 541 k × g for 1 h; Beckman Coulter, Miami, FL).

3. Results

3.1. Identification of SEC14L1a as a potential regulator of HIV-1 replication

We prepared MT-4 cells that constitutively express cDNA transduced by a lentiviral vector or an MLV-based retroviral vector (Fig. 1A). The cDNAs were derived from human peripheral blood mononuclear cells (PBL) and *Oryctolagus cuniculus* (European rabbit) kidney-derived cell line RK13 cells. MT-4 cells transduced with cDNA were collected by FACS sorter using the green fluorescence as a marker since viral vectors encoded the GFP expression cassette. Then, cells were infected with HIV-1. Surviving cells were propagated and the genomic DNA was extracted to recover the transduced cDNA by PCR as previously described [3]. We isolated two clones encoding the carboxy terminal domain (CTD) of SEC14L1a (Gene ID 6397, Fig. 1B and C); one from the PBL cDNA library (1/65 independent clones, 1.5%), and one from the RK13 cDNA library (1/42 independent clones, 2.4%). The fact that the SEC14L1a CTD was successfully identified from two independent cDNA libraries strongly suggests that it is a negative regulator of HIV-1 replication. It is important to note that previous genome-wide screenings for HIV-1 regulators have not identified SEC14L1a CTD. This clearly suggests that our T cell-based cDNA screening system is unique, and should be able to complement the other genome-wide screening systems.

SEC14L1a belongs to the widely-expressed SEC14-superfamily that is involved in membrane trafficking and phospholipid metabolism [18–21]. The function of SEC14L1a is not well understood. The C-terminus of SEC14L1a encodes a Golgi dynamics (GOLD) domain (amino acids (aa) 523–674; Fig. 1C) that mediates the protein-protein interaction possibly involved in the maintenance of Golgi apparatus function and vesicular trafficking [22]. The only reported biological activity of SEC14L1a is to interact with cholinergic receptors AchT and CHT1 [23]. The GOLD domain is responsible for the physical interaction between SEC14L1a and cholinergic receptors. However, the functional significance of these interactions remains to be clarified. The conserved SEC14 domain directly interacts with lipid molecules [17–21]. However, the lipid ligand of SEC14L1a (aa 319–490, Fig. 1C) has yet to be identified.

3.2. Construction of expression vectors for SEC14L1a derivatives

The longest SEC14L1a cDNA recovered from the PBL cDNA library spanned nucleotides (nt) 2045–2492 of SEC14L1a mRNA (NM_003003.3), covering the CTD of the SEC14L1a open reading frame (ORF; Fig. 1B). We detected a potential translational start codon at nt 2188-2190 within the GOLD domain (asterisk, Fig. 1B). We speculated that the isolated cDNA might have expressed the carboxy half of the GOLD domain (aa 641–715) in MT-4 cells, leading to the inhibition of HIV-1 replication.

To test this, we constructed an expression plasmid for FLAG-tagged CTD (aa 642-715) fused to the carboxy terminus of GFP (CTD1; Fig. 1C). We also constructed GFP fusion proteins spanning the GOLD domain (CTD2, aa 493–715) or the full-length SEC14L1a (FL; Fig. 1C). Expression of these proteins was verified by Western blotting of transient transfected 293T cells (Fig. 1D). The confocal microscopy analysis indicated that the FL localized mainly in the cytoplasm, with some accumulation in the perinuclear regions (Fig. 1E), consistent with a previous report [23]. CTD1 was distributed in the cytoplasm and the nucleus, with a slight preference for the cytoplasm. CTD2 was evenly distributed to the nucleus and cytoplasm. When MT-4 cells constitutively expressing FL, CTD1, and CTD2 were analyzed, the subcellular distribution was less clear, due to the small cytoplasm of the cells (Fig. 1F). However, FL was distributed evenly to the nucleus and cytoplasm in MT-4 cells. In contrast, CTD1 was excluded from the nucleus in MT-4 cells (Fig. 1F). The distribution of CTD2 in MT-4 cells was similar to that in 293T cells (Fig. 1F). The differences of protein distribution in two cell types may be caused by the cell type-dependent regulation of protein trafficking and/or the effect of protein expression levels.

3.3. Verification of anti-HIV-1 activity associated with SEC14L1a CTD1

We introduced FL, CTD1, or CTD2 into MT-4 cells using the MLV vector, and isolated cells constitutively expressing FL, CTD1, or CTD2. Expression of SEC14L1a derivatives in MT-4 cells was verified by Western blotting (Fig. 2A). FL expression was verified by immuno-precipitation assay (Fig. 2A). The detection of FL by Western blotting was inefficient considering the fact that all the SEC14L1a derivatives are GFP-tagged, and the GFP intensity of FL-expressing MT-4 cells was not lower than that of CTD1-expressing
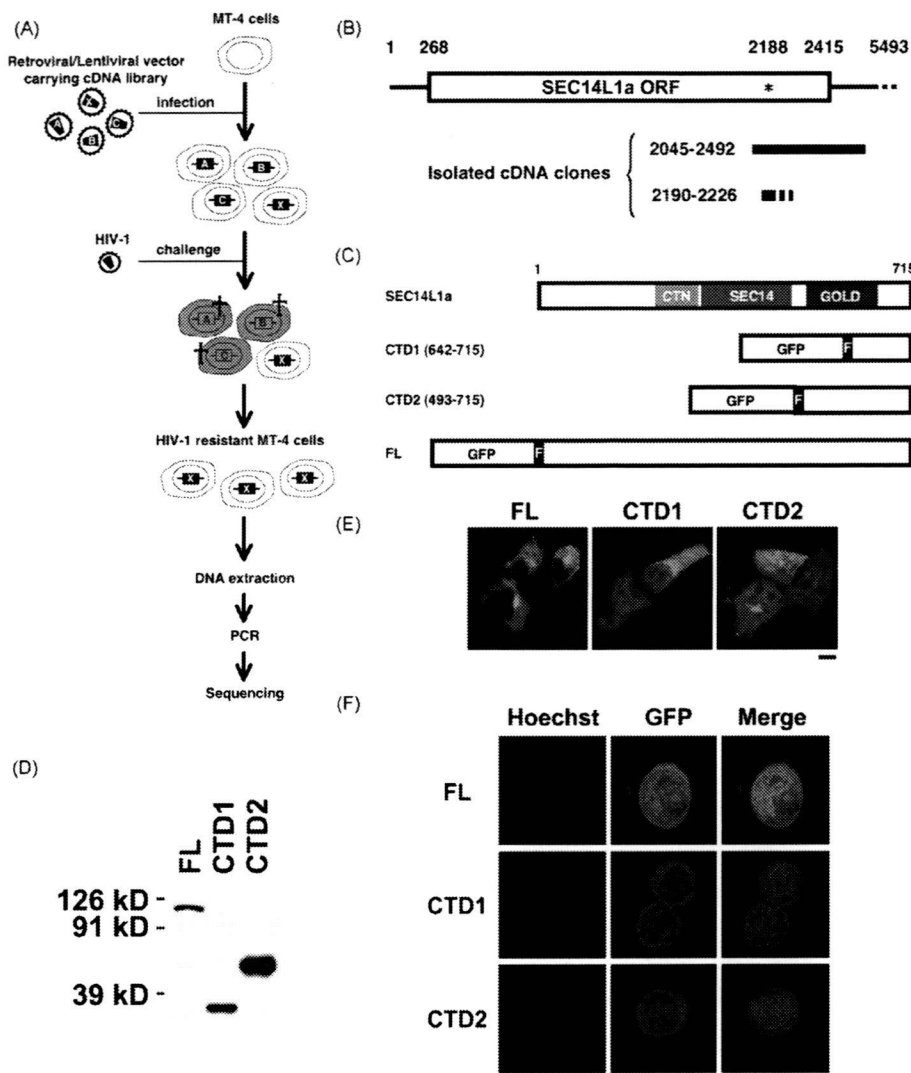
4   E. Urano et al. / Vaccine xxx (2009) xxx–xxx

Fig. 1. Identification of SEC14L1a CTD as a potential regulator of HIV-1 replication. (A) The experimental strategy used to screen a cDNA library for genes rendering cells resistant to HIV-1. MT-4 cells were infected with a retroviral or lentiviral vector carrying cDNA libraries and were challenged with wild-type HIV-1$_{HXB2}$. The HIV-1-infected cells (gray with cross) quickly undergo cell death. The surviving cells were propagated, collected, and the transduced cDNA labeled X was determined. (B) Schematic representation of SEC14L1a mRNA (NM_00303.3) and the isolated gene fragments. The open reading frame (ORF) is assigned from nucleotides (nt) 268 to 2415. The potential internal translational initiation codon is marked with an asterisk. (C) Schematic representation of the SEC14L1a protein (NP_002994). SEC14L1a has a CRAL_TRIO_N domain (CTN, amino acids 241–313), a SEC14p-like lipid-binding domain (SEC14, amino acids 319–490), and a Golgi dynamics domain (GOLD, amino acids 523–674). The cloned fragments (CTD1 and CTD2) and full-length (FL) gene were tagged with a FLAG epitope (indicated with an "F") on their N-termini, and fused to the C-terminus of GFP. (D) Verification of FL, CTD1, and CTD2 expression in 293T cells by Western blotting using anti-FLAG antibody. (E) Confocal microscopy images of 293T cells expressing FL, CTD1, or CTD2. The green signal represents GFP fluorescence. Magnification, 630×; scale bar, 10 μm. (F) Confocal microscopy images of MT-4 cells constitutively expressing FL, CTD1, or CTD2. The blue signal represents the Hoechst-stained nucleus, and green represents GFP fluorescence. Magnification, 630×; scale bar, 5 μm.

cells (Fig. 1F). The MLV vector expressing GFP alone was used as a control. The cell proliferation, morphology, and cell surface levels of HIV-1 receptors were unaltered by any of the SEC14L1a derivatives (Fig. 1F, 2B, and data not shown). HIV-1 replication was tested in these cells. The level of HIV-1 replication was significantly inhibited in CTD1- and CTD2-expressing cells (69.1% and 69.8% on the average from seven independent experiments, respectively, $P < 0.05$, two-tailed Student's t-test), but was hardly inhibited in FL-expressing cells (86.4%, not statistically significant; Fig. 2C). This observation was reproducible in independently established MT-4 cells and SupT1 cells (data not shown). These data verified the original screening results, and suggest that the C-terminal half

of GOLD domain of SEC14L1a serves as an inhibitor of HIV-1 replication. In contrast, it is suggested that FL is not a potent negative regulator of HIV-1 replication.

3.4. SEC14L1a CTD1 and CTD2 target the late phase of the HIV-1 life cycle

We analyzed the viral entry and production phases to determine which step of the HIV-1 life cycle CTD1 and CTD2 target.

The Alu-LTR PCR assay was performed to examine the effect of SEC14L1a derivatives on the viral entry phase. The MT-4 cells stably expressing GFP, FL, CTD1, or CTD2 were infected with VSV-
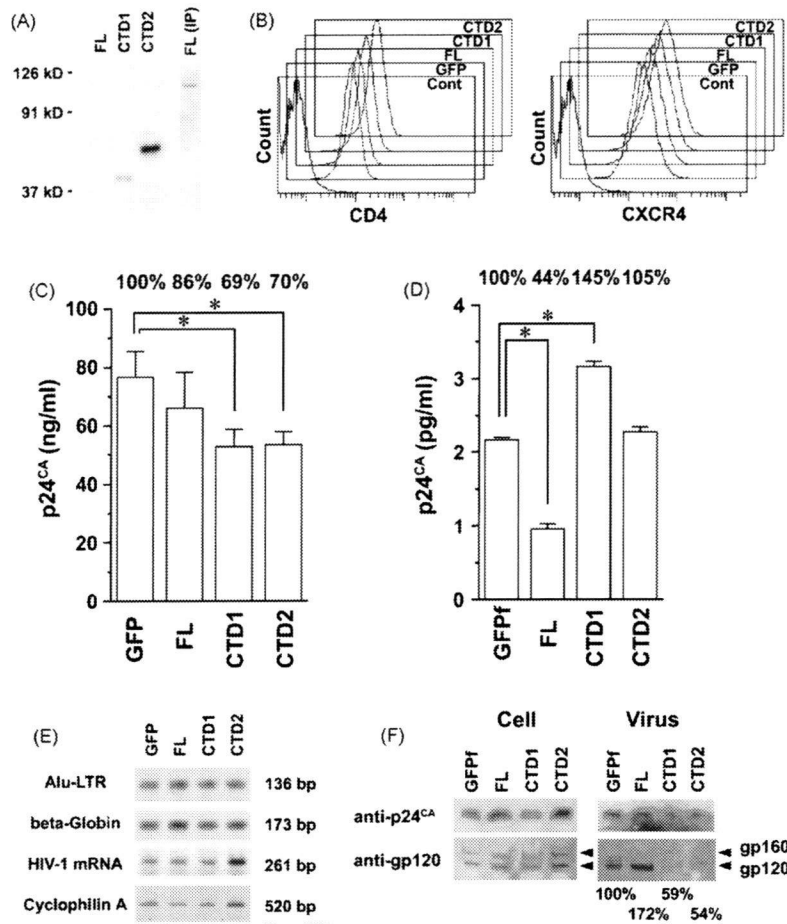
Fig. 2. Functional characterization of the SEC14L1a derivatives. (A) Detection of stable expression of FL, CTD1, and CTD2 in MT-4 cells by Western blotting using anti-FLAG antibody. FL was detected by the immunoprecipitation (IP) assay using agarose beads conjugated with anti-FLAG antibody. The flow cytometric analysis of the cell surface expression of HIV-1 receptors CD4 and CXCR4 in MT-4 cells stably expressing GFP, FL, CTD1, and CTD2. (C) Constitutive expression of CTD1 and CTD2 limited the replication of HIV-1 in MT-4 cells. The concentration of viral p24^{CA} antigen in the culture supernatant was measured at 4 d post-infection. The results represent the average of seven independent experiments ± the standard error of the mean. The reduction of viral p24^{CA} concentration relative to GFP was shown on the top. Asterisks indicate the statistical significance compared to GFP ($P < 0.05$ by two-tailed Student's t-test). (D) The PCR-based assay to examine the effect of SEC14L1a derivatives on the early phase of viral life cycle (top two panels) and the transcription from LTR promoter (bottom two panels). The HIV-1 entry efficiency was examined by Alu-LTR PCR. Beta globin was used as an internal control. The HIV-1 transcription efficiency was examined by RT-PCR targeting spliced viral mRNA. Cyclophilin A was used as a control. The expected length of each PCR amplicon was indicated. (E) The effect of SEC14L1a derivatives on the HIV-1 production. The 293T cells grown in a well of a 6-well plate were transfected with 200 ng of HIV-1 proviral DNA and 2 μg of expression vector for GFPf, FL, CTD1, or CTD2. The culture supernatant was recovered at 2 d post-transfection and the p24^{CA} concentration was measured. The representative data from five independent experiments was shown. The results indicate the average ± the standard deviation. The relative p24^{CA} concentration compared to GFPf was shown on the top. Asterisks indicate the statistical significance compared to GFPf ($P < 0.001$ by two-tailed Student's t-test). The Env incorporation onto the virus-like particles (VLP) produced by 293T cells expressing SEC14L1a derivatives. The 293T cells grown in a well of a 6-well plate were transfected with 1 μg of gag-pol (pCMVR8.91) and Env (pIIIex) expression vectors along with 2 μg of expression vector for GFPf, FL, CTD1, or CTD2. The cell lysates (Cell) and VLP fractions (Virus) were subjected to Western blot analysis detecting gp120 and p24^{CA} harvested at 2 d post-transfection. The Env incorporation levels normalized to p24^{CA} relative to GFPf were shown at the bottom.

G-pseudotyped HIV-1 vector, and the cellular genomic DNA was recovered at 4 d post-infection. The amount of Alu-LTR PCR products from FL-, CTD1-, or CTD2-expressing MT-4 cells was almost equal to that from GFP-expressing cells, suggesting that the early phase of the viral life cycle is not inhibited by any of the SEC14L1a derivatives (Fig. 2D). To examine the viral production phase, we examined the LTR-driven viral gene transcription by RT-PCR. Cellular RNA was extracted from the same MT-4 cells infected with VSV-G-pseudotyped HIV-1 vector, and RT-PCR was conducted to amplify LTR promoter-driven spliced HIV-1 mRNA. The amount of viral RNA expressed in FL-, CTD1-, or CTD2-expressing cells was not lower than that in GFP-expressing cells when the levels of the internal control was taken into account (Fig. 2D). Given that the similar number of viral genome was integrated as indicated by the

Alu-LTR PCR, these data suggest that viral transcription is not inhibited by any of the SEC14L1a derivatives, and that the action point of CTD1 and CTD2 should be at post-transcriptional levels of the viral production phase.

Next, the FL, CTD1, or CTD2 expression vector was co-transfected with HIV-1 proviral DNA into 293T cells, and viral production was quantified by p24^{CA} ELISA. The FLAG-tagged GFP (GFPf) was used as a control hereafter. We found that the FL expression significantly reduced the production of HIV-1 (44.2%, $P < 0.001$, two-tailed Student's t-test) compared to the GFPf control (Fig. 2E). In contrast, the CTD1 enhanced the production of HIV-1 (145.9%, $P < 0.001$, two-tailed Student's t-test; Fig. 2E). However, CTD2 did not measurably affect the HIV-1 production (105.1%, not statistically significant; Fig. 2E). As the ELISA assay examines the effect

of CTDs on *Gag* functions, we next tested the functional interaction between CTDs and *Env*. The *Env* incorporation onto the virion was examined by tripartite-transfection of expression vectors for *Env*, *gag-pol*, and SEC14L1a derivatives into 293T cells, and the VLP was collected by centrifugation. The immunoblotting against gp120 was performed on the cell lysate and the VLP fraction. The cellular *Env* and *Gag* expressions were not detectably affected by any of the SEC14L1a derivatives (Fig. 2F, left panel). The *Env* incorporation onto the VLP was slightly enhanced by FL (157%; Fig. 2F, right panel). In contrast, the VLP produced from CTD1- or CTD2-expressing cells incorporated substantially fewer *Env* than those from GFPf-expressing cells (59% or 54%, respectively; Fig. 2F, right panel). These data were reproducible in independently performed experiments. The densitometric analysis of Western blot image showed that the average ± the standard error of the mean of Env incorporation onto the virion was $129.7 \pm 39.9\%$, $54.8 \pm 24.7\%$, and $25.5 \pm 10.3\%$ for FL, CTD1, and CTD2 compared to GFPf, respectively (3–4 independent experiments). The *Env*-mediated cell-to-cell fusion assay indicated that SEC14L1a derivatives did not limit the cell surface targeting and function of *Env* (data not shown). In addition, the *Gag* processing in virion was unaffected by any of the SEC14L1a derivatives (data not shown). Collectively, these data suggest that the HIV-1 replication is inhibited by CTD1 and CTD2 due to the inefficient *Env* incorporation onto the virion. To test this possibility, we infected fresh MT-4 cells with the equal amount of HIV-1 propagated in CTD1- or CTD2-expressing MT-4 cells (1–2 ng p24^{CA}), and the viral replication was monitored at 3–4 days post-infection by measuring the p24^{CA} concentration. The infectivity of HIV-1 propagated in CTD1- or CTD2-expressing cells was attenuated to $83.1 \pm 17.9\%$ or $82.4 \pm 5.5\%$ relative to the virus recovered from GFP-expressing cells, respectively (the average ± the standard error of the mean of 3 independent experiments). Altogether, these data suggest that the inhibition of HIV-1 replication by CTD1 and CTD2 is attributed to the attenuation of viral infectivity by lowering the *Env* incorporation onto the virion.

4. Discussion

In the present study, we provide the first evidence that the C-terminal fragment of SEC14L1a functions as an inhibitor of HIV-1 replication. The advantage of this system is that, since MT-4 cells are stably transduced with a cDNA library, the anti-HIV-1 function of a candidate gene is not due to a perturbed cell physiology. This system has been successful in identifying CD14, CD63, and Brd4-CTD as regulators of HIV-1 replication [1,3,4], and more candidates are being analyzed. Among the candidates, SEC14L1a CTD appeared to be one of the relatively modest inhibitors of HIV-1 replication. However, of note, the SEC14L1a derivatives have not been identified in other genetic screening systems. These facts point that our T cell-based system is sensitive in detecting the modest anti-HIV-1 activity of a gene, and is a unique tool in the pursuit of HIV-1 regulatory factors to complete the HIV-1-host interactome.

SEC14L1a may affect the Golgi-mediated vesicular trafficking since SEC14L1a lowers the cell surface levels of cholinergic transporters [23]. However, we do not have any data to suggest that SEC14L1a and its derivatives affect the cell surface targeting of membrane proteins including CD4, CXCR4 and *Env*. These data suggest that SEC14L1a's effect on cholinergic receptor expression is specific, and that the CTD's ability to inhibit HIV-1 replication is independent from SEC14L1a's regulatory functions on vesicular trafficking. The action point of CTD1 and CTD2 was shown to be the late phase of the viral life cycle. Given that CTD1 and CTD2 did not inhibit the biogenesis and the cell surface targeting of *Gag* and *Env*, the major mechanism of CTD1 and CTD2 to inhibit HIV-1 replication was to reduce the infectivity of HIV-1 by limiting the *Env* incorporation onto the virion. Consistent with this idea, the

viral infectivity of virions produced in CTDs-expressing cells was attenuated. Then, how do CTDs block the *Env* incorporation onto the virion? We detected a weak interaction between *Gag* and CTD1 or CTD2 by immuno-coprecipitation analysis. Thus, we speculate that the interaction between *Env* and *Gag* at the plasma membrane is interfered by *Gag*-CTDs interaction, resulting in the reduction of *Env* incorporation onto the virion.

The CTD1 was an inhibitor of HIV-1 replication. While the CTD1 negatively affected the *Env* incorporation onto the virion, it positively affected the HIV-1 production. These observations may be seemingly controversial. However, the SEC14L1a derivatives' effect on HIV-1 replication is a summation of their effects of on each step of the viral life cycle. Therefore, it is conceivable that CTD1 can serve as a negative regulator of HIV-1 replication as well as a positive and negative factor on distinct steps of the viral life cycle. These seemingly controversial findings may be in part due to the cells in which the biological functions of SEC14L1a derivatives were examined. The effect of SEC14L1a derivatives on HIV-1 replication was investigated in MT-4 cells, whereas those on the HIV-1 production and *Env* incorporation onto the virion were examined in 293T cells. Although the basic biological features are largely shared among different cell types, it is possible that the SEC14L1a derivatives may function slightly differently in MT-4 cells from 293T cells given that the intracellular distribution of SEC14L1a derivatives in MT-4 cells was not identical to that in 293T cells (Fig. 1E and 1F).

Elucidating the molecular mechanism underlying CTDs' activity not only provides a hint to understand how the HIV-1 virion actively uptakes *Env* through the *Gag-Env* interaction, but also leads to the development of a novel anti-retroviral drug that lowers the infectivity of the virus by preventing *Env* incorporation onto the virion. This is the strength of our T cell-based assay since CTDs inhibit HIV-1 replication specifically. In the previous study, we proposed that a small portion of Brd4 may serve as a therapeutic molecular target for HIV-1 infection, since the constitutive expression of Brd4-CTD limited HIV-1 replication specifically [3], akin to the SEC14L1a CTDs. However, it remains to be examined whether the SEC14L1a and Brd4 derivatives inhibit HIV-1 replication in primary HIV-1 target cells.

The genome-wide screening has potential caveats, including a cDNA bias and a cell line bias. A cDNA library is not a perfect representation of mRNA expressed in the cells from which the library is constructed. For example, the longer the mRNA, the less efficiently the full-length cDNA is synthesized. In fact, we isolated Brd4-CTD from the PBL cDNA library as a potent inhibitor of HIV-1 replication [3]. However, although Brd4 (approximately 5000 nt mRNA in length) is expressed in MT-4 cells, we were unable to recover Brd4-CTD from the MT-4 cDNA library [3]. This clearly demonstrates the cDNA bias in the genetic screening. A cDNA library derived from non-T cells does not contain genes specifically expressed in T cells. Thus, we have to explore many more cDNA libraries to completely cover the genetic diversity of human cells. The cDNA libraries isolated from long-term non-progressors of HIV-1-seropositive individuals or from elite controllers might be of particular interest, considering that a dominant innate HIV-1 resistance gene, such as CCR5 delta 32, may partly account for the slow progression of AIDS. Similarly, use of a particular cell line and/or virus strain may bias the results. MT-4 cells are positive for HTLV-1, and are able to support robust HIV-1 replication. MT-4 cells do not express CCR5, and are unable to support R5-tropic HIV-1 strains. What if other T cell lines and R5-tropic viral strains are used? What if we assay the same cDNA library in TZM-bl cells? We plan to address these issues in the future studies.

In conclusion, genome-wide genetic screening is a powerful tool for identifying the regulatory factors of HIV-1 replication and innate HIV-1 resistance factors that limit HIV-1 infection and AIDS progression. The HIV-1-host interactome should also reveal poten-

tial therapeutic molecular targets that may be used to develop novel anti-AIDS drugs to tackle the emerging drug resistant viruses. However, the fact that different experimental systems often yield non-overlapping candidates suggests that we have to explore more experimental systems to fully understand the HIV-1-host interactome. Our T cell-based system provides an alternative tool for identifying novel HIV-1 regulatory factors, and should help us understand the HIV-1-host interaction in more detail.

Acknowledgements

References

[1] Kawano Y, Yoshida T, Hieda K, Aoki J, Miyoshi H, Koyanagi Y. A lentiviral cDNA library employing lambda recombination used to clone an inhibitor of human immunodeficiency virus type 1-induced cell death. J Virol 2004;78(20):11352–9.
[2] Valente ST, Goff SP. Inhibition of HIV-1 gene expression by a fragment of hnRNP U. Mol Cell 2006;23(4):597–605.
[3] Urano E, Kariya Y, Futahashi Y, Ichikawa R, Hamatake M, Fukazawa H, et al. Identification of the P-TEFb complex-interacting domain of Brd4 as an inhibitor of HIV-1 replication by functional cDNA library screening in MT-4 cells. FEBS Lett 2008;582(29):4053–8.
[4] Yoshida T, Kawano Y, Sato K, Ando Y, Aoki J, Miura Y, et al. A CD63 mutant inhibits T-cell tropic human immunodeficiency virus type 1 entry by disrupting CXCR4 trafficking to the plasma membrane. Traffic 2008;9(4):540–58.
[5] Zhou H, Xu M, Huang Q, Gates AT, Zhang XD, Castle JC, et al. Genome-scale RNAi screen for host factors required for HIV replication. Cell Host Microbe 2008;4(5):495–504.
[6] Brass AL, Dykxhoorn DM, Benita Y, Yan N, Engelman A, Xavier RJ, et al. Identification of host proteins required for HIV infection through a functional genomic screen. Science 2008;319(5865):921–6.
[7] Konig R, Zhou Y, Elleder D, Diamond TL, Bonamy GM, Irelan JT, et al. Global analysis of host-pathogen interactions that regulate early-stage HIV-1 replication. Cell 2008;135(1):49–60.
[8] Valente ST, Gilmartin GM, Mott C, Falkard B, Goff SP. Inhibition of HIV-1 replication by eIF3f. Proc Natl Acad Sci USA 2009;106(11):4071–8.
[9] Aiken C. Pseudotyping human immunodeficiency virus type 1 (HIV-1) by the glycoprotein of vesicular stomatitis virus targets HIV-1 entry to an endocytic pathway and suppresses both the requirement for Nef and the sensitivity to cyclosporin A. J Virol 1997;71(8):5871–7.
[10] Akari H, Uchiyama T, Fukumori T, Iida S, Koyama AH, Adachi A. Pseudotyping human immunodeficiency virus type 1 by vesicular stomatitis virus G protein does not reduce the cell-dependent requirement of vif for optimal infectivity: functional difference between Vif and Nef. J Gen Virol 1999;80(Pt 11):2945–9.
[11] Chazal N, Singer G, Aiken C, Hammarskjold ML, Rekosh D. Human immunodeficiency virus type 1 particles pseudotyped with envelope proteins that fuse at low pH no longer require Nef for optimal infectivity. J Virol 2001;75(8):4014–8.
[12] Komano J, Miyauchi K, Matsuda Z, Yamamoto N. Inhibiting the Arp2/3 complex limits infection of both intracellular mature vaccinia virus and primate lentiviruses. Mol Biol Cell 2004;15(12):5197–207.
[13] Goff SP. Knockdown screens to knockout HIV-1. Cell 2008;135(3):417–20.
[14] Urano E, Aoki T, Futahashi Y, Murakami T, Morikawa Y, Yamamoto N, et al. Substitution of the myristoylation signal of human immunodeficiency virus type 1 Pr55Gag with the phospholipase C-delta1 pleckstrin homology domain results in infectious pseudovirion production. J Gen Virol 2008;89(Pt 12):3144–9.
[15] Futahashi Y, Komano J, Urano E, Aoki T, Hamatake M, Miyauchi K, et al. Separate elements are required for ligand-dependent and -independent internalization of metastatic potentiator CXCR4. Cancer Sci 2007;98(3):373–9.
[16] Zufferey R, Dull T, Mandel RJ, Bukovsky A, Quiroz D, Naldini L, et al. Self-inactivating lentivirus vector for safe and efficient in vivo gene delivery. J Virol 1998;72(12):9873–80.
[17] Shimizu S, Urano E, Futahashi Y, Miyauchi K, Isogai M, Matsuda Z, et al. Inhibiting lentiviral replication by HEXIM1, a cellular negative regulator of the CDK9/cyclin T complex. AIDS 2007;21(5):575–82.
[18] Chinen K, Takahashi E, Nakamura Y. Isolation and mapping of a human gene (SEC14L), partially homologous to yeast SEC14, that contains a variable number of tandem repeats (VNTR) site in its 3' untranslated region. Cytogenet Cell Genet 1996;73(3):218–23.
[19] Howe AG, McMaster CR. Regulation of phosphatidylcholine homeostasis by Sec14. Can J Physiol Pharmacol 2006;84(1):29–38.
[20] Saito K, Tautz L, Mustelin T. The lipid-binding SEC14 domain. Biochim Biophys Acta 2007;1771(6):719–26.
[21] Mousley CJ, Tyeryar KR, Vincent-Pope P, Bankaitis VA. The Sec14-superfamily and the regulatory interface between phospholipid metabolism and membrane trafficking. Biochim Biophys Acta 2007;1771(6):727–36.
[22] Anantharaman V, Aravind L. The GOLD domain, a novel protein module involved in Golgi function and secretion. Genome Biol 2002;3(5), research0023.0021-0023.0027.
[23] Ribeiro FM, Ferreira LT, Marion S, Fontes S, Gomez M, Ferguson SS, et al. SEC14-like protein 1 interacts with cholinergic transporters. Neurochem Int 2007;50(2):356–64.

Dominant-negative derivative of EBNA1 represses EBNA1-mediated transforming gene expression during the acute phase of Epstein–Barr virus infection independent of rapid loss of viral genome

Yumi Kariya,[1,2] Makiko Hamatake,[1] Emiko Urano,[1] Hironori Yoshiyama,[3] Norio Shimizu[2] and Jun Komano[1,4]

[1]AIDS Research Center, National Institute of Infectious Diseases, Tokyo; [2]Department of Virology, Division of Medical Science, Medical Research Institute, Tokyo Medical and Dental University, Tokyo; [3]Research Center for Infection-associated Cancer, Institute for Genetic Medicine, Hokkaido University, Sapporo, Japan

The oncogenic human herpes virus, the Epstein–Barr virus (EBV), expresses EBNA1 in almost all forms of viral latency. EBNA1 plays a major role in the maintenance of the viral genome and in the transactivation of viral transforming genes, including EBNA2 and latent membrane protein (LMP-1). However, it is unknown whether inhibition of EBNA1 from the onset of EBV infection disrupts the establishment of EBV's latency and transactivation of the viral oncogenes. To address this, we measured EBV infection kinetics in the B cell lines BALL-1 and BJAB, which stably express a dominant-negative EBNA1 (dnE1) fused to green fluorescent protein (GFP). The EBV genome was surprisingly unstable 1 week post-infection: the average loss rate of EBV DNA from GFP- and GFP-dnE1-expressing cells was 53.4% and 41.0% per cell generation, respectively, which was substantially higher than that of an 'established' oriP replicon (2–4%). GFP-dnE1 did not accelerate loss of the EBV genome, suggesting that EBNA1-dependent licensing of the EBV genome occurs infrequently during the acute phase of EBV infection. In the subacute phase, establishment of EBV latency was completely blocked in GFP-dnE1-expressing cells. In contrast, C/W promoter-driven transcription was strongly restricted in GFP-dnE1-expressing cells at 2 days post-infection. These data suggest that inhibition of EBNA1 from the onset of EBV infection is effective in blocking the positive feedback loop in the transactivation of viral transforming genes, and in eradicating the EBV genome during the subacute phase. Our results suggest that gene transduction of GFP-dnE1 could be a promising therapeutic and prophylactic approach toward EBV-associated malignancies. (*Cancer Sci* 2010)

The Epstein–Barr virus (EBV) is a risk factor in several malignant diseases including Burkitt's lymphoma and nasopharyngeal carcinoma.[1–4] The opportunistic B-cell lymphoma is becoming the major cause of death in AIDS patients in an era of highly active antiretroviral therapy (HAART), and EBV is associated with a significant portion of AIDS lymphoma cases.[5,6] Neither an EBV vaccine, nor specific antiviral agents against EBV are available; thus attention should be paid to the development of therapeutic agents against EBV.

EBV-encoded genes including EBNA1, EBNA2, and latent membrane protein (LMP-1) are potential molecular targets for the treatment of EBV-associated lymphomas because they play central roles in the process of malignant transformation.[7] We are interested in EBNA1 since it contributes to EBV oncogenesis in two ways: it supports the maintenance of the EBV genome in *cis* and enhances expression of viral oncogenes, including EBNA2 and LMP-1, in *trans*.[7–9] EBNA1 exerts its biological functions by binding to its cognate binding sites within the family of repeats (FR) and the dyad symmetry element (DS) located within the origin of replication (oriP) of EBV DNA. EBNA1 interacts with FR to enhance transcription from the viral C/W promoters (C/Wp) and to partition EBV DNA to daughter cells; and with DS to initiate DNA replication.[7–9]

Maintenance of the oriP replicon is stable once EBV latency has been established. The loss rate of established oriP plasmids is estimated at 2–4% per cell generation.[10,11] Interestingly, the loss rate of the oriP replicon is significantly higher in cells transiently transduced with oriP plasmids (>25% per cell generation) than in established cells.[12] In primary B cells, EBV DNA is lost rapidly within 2 days post-infection (~98.9%).[13] However, the loss rate of the EBV genome during a week post-infection in B cells remains to be quantified.

Upon EBV infection, the first viral genes expressed are the transactivators EBNA2 and EBNA-LP transcribed from Wp several hours after infection.[7] EBNA2 binds to the EBNA2-responsive elements and, in cooperation with EBNA-LP, enhances transcription from Cp, which leads to expression of all EBNA proteins, including EBNA1. EBNA1 binding to oriP activates C/Wp to boost viral latent gene expression, including the EBNAs and LMP-1. The viral gene transactivation positive feedback loop is established within a few days post-infection, and EBNA1 is one of the key factors that sustain this feedback loop during the acute phase of EBV infection.[14] In parallel, EBNA1 contributes to the establishment of the EBV genome as a licensed replicon. It may be possible to stop EBV infection by breaking the chain of EBNA1-dependent events and thus the EBV-mediated malignant transformation of infected cells. Previous studies have assessed the therapeutic potential of a dominant-negative derivative of EBNA1 (dnE1) in cells in which EBV latency was already established.[15,16] In this study, we critically assessed whether inhibition of EBNA1 limits the early stage of EBV infection in B cells. We provide evidence that expression of dnE1 strongly blocks the expression of virus-encoded oncogenes in acutely infected cells without accelerating EBV genome loss, and disrupts EBV latency in the subacute phase of EBV infection.

Materials and Methods

Cells. The 293T, EBV-negative Burkitt lymphoma cell line BJAB, EBV-positive Burkitt lymphoma cell line Daudi, EBV-transformed healthy donor-derived B lymphoblastoid cell line (B-LCL), and B acute lymphoblastic leukemia cell line BALL-1

---

[4]To whom correspondence should be addressed.
E-mail: ajkomano@nih.go.jp

cells (kindly provided by Dr. Yokota, National Institute of Infectious Diseases, Tokyo, Japan) were maintained in RPMI-1640 medium (Sigma, St. Louis, MA, USA) supplemented with 10% fetal bovine serum (Japan Bioserum, Tokyo, Japan), 50 U/mL penicillin, 50 μg/mL streptomycin (Invitrogen, Tokyo, Japan), and incubated at 37°C in a humidified 5% CO_2 atmosphere.

Plasmids. The following primers were used to amplify dnE1 from p1160[17] by PCR: 5′-ACCGGTCTCGAGCAATTGCCA-CCATGCGGGGTCAGGGTGATGGAGG-3′ and 5′-GGATC-CTCGAGCGGCCGCTCACTCCTGCCCTTCCTCACC-3′. The GFP-dnE1 expression vector (pGD) was constructed by cloning the MfeI-XhoI fragment of the PCR product into the BglII-SalI sites of pEGFP-C1 (Clontech, Palo Alto, CA, USA). The MfeI and BglII sites were blunted with T7 RNA polymerase. The AgeI-BamHI fragment from pGD was cloned into the corresponding restriction sites of pCMMP eGFP[15,18] to generate pCMMP GFP-dnE1. The EBNA1 expression vector p1553, the FR-tk-luciferase reporter p985, and pLuciferase (pCMV-luc) have been described previously.[17–20]

Luciferase assay. The 293T cells, grown in 48-well plates, were co-transfected with the indicated plasmids using Lipofecta-mine 2000 according to the manufacturer's protocol (Invitrogen, Tokyo, Japan). Cells were replated in 96-well plates in triplicate at 2 h post-transfection. Luciferase activity was measured 48 h after transfection using the Steady-Glo Kit (Promega, Madison, WI, USA).

Murine leukemia virus (MLV) vector infection and cell sorting. MLV vectors were produced as described previously.[18] B cells (1×10^7 cells) were incubated with 2 mL of MLV preparation overnight at 4°C with continuous agitation. GFP-positive cells were collected using a FACS sorter (FACS Vantage; Becton Dickinson, San Jose, CA, USA) at 11 days post-infection.

Western blotting. Western blotting was performed as described previously.[21,22] The following reagents were used: anti-GFP (MsX Green Fluorescent Protein; Chemicon, Temecula, CA, USA) and Envision⁺ Dual Link System-HRP (Dako, Glostrup, Denmark).

EBV infection and nucleic acid extraction. The EBV B95-8 strain was a generous gift from Dr Fujiwara's group at the National Research Institute for Child and Development (Tokyo, Japan). B cells (1×10^7 cells) were incubated with 100 μL of B95-8 EBV for 1 h at 37°C, and genomic DNA was extracted from half of the infected cells soon after infection (QIAamp DNA Mini Kit; Qiagen, Tokyo, Japan). At 15 h post-infection, half of the cells were washed once with PBS and incubated for 5 min in lysis buffer (10 mM Tris-HCl [pH7.4], 10 mM NaCl, 3 mM $MgCl_2$, and 0.5% NP-40). The nuclear fraction was collected by centrifugation for 5 min at 20.6 K × g (Kubota 3740; Kubota, Tokyo, Japan), and high molecular weight DNA was extracted (nuclear DNA). At 2 days post-infection and at later time points, high molecular weight DNA, or total RNA (Pure-Link Total RNA Blood Purification Kit; Invitrogen) was extracted from 1×10^6 or 3×10^6 cells, respectively, according to the manufacturer's protocol. After EBV infection, 10 μM aciclovir (Kayaku, Tokyo, Japan) was added to the culture medium. The production and infection of the recombinant EBV Akata strain carrying GFP and neomycin resistant genes has been described previously.[23] At 2 days post-infection, cells were plated at a density of 1×10^4 cells per well in a flat-bottomed 96-well plate, and cultured in a medium containing 1 mg/mL G418. The efficiency of EBV latency establishment was evaluated as percentage of wells positive for the emergence of G418-resistant cells at 2 to 3 weeks post-G418 selection.

Quantitative real-time PCR. Real-time PCR was performed as described previously; serial dilutions of positive controls were used as standards.[21] Amplifications were performed using the

QuantiTect SYBR Green RT-PCR/PCR Kit (Qiagen), and the following primers: BamHI W repeat, 5′-GCCAGAGG-TAAGTGGACTTT-3′ and 5′-AGAAGCATGTATACTAAGC-CTCCC-3′; cyclophilin A (CYPA), 5′-CACCGCCACCATG-GTCAACCCCA-3′ and 5′-CCCGGGCCTCGAGCTTTCGAG-TTGTCCACAGTCAGCAATGG-3′; C/Wp, 5′-CCCTCGGA-CAGCTCCTAAG-3′ and 5′-CTTCACTTCGGTCTCCCCTA-3′; EBER1, 5′-AAAACATGCGGACCACCAGC-3′ and 5′-AG-GACCTACGCTGCCCTAGA-3′. The β-globin primers were described previously.[21] Following PCR amplification, the amplicons were separated in a 2% agarose gel, stained with ethidium bromide, and imaged with a Typhoon scanner (GE Healthcare Bio-Sciences; Piscataway, NJ, USA).

Results

Construction and functional verification of dnE1 fused to GFP. The carboxy half of EBNA1 serves as a functional dominant-negative inhibitor of EBNA1 that restricts the replication and maintenance of oriP plasmids as well as the EBNA1-dependent enhancement of transcription.[17,24] We used a dnE1 mutant encompassing amino acids 377 to 391 (the nuclear localization signal, NLS) and 451 to 641 (the DNA binding and dimerization domain) of EBNA1 (Fig. 1A).[17] To visualize the intracellular distribution of dnE1, we constructed the retroviral expression vector encoding GFP-dnE1. The expression of GFP-dnE1 was verified in transiently transfected 293T cells and stably transduced B cell lines using an MLV vector. To verify the function of GFP-dnE1, we conducted a reporter assay using a plasmid encoding the FR-tk-luciferase cassette. EBNA1 enhances expression of FR-tk-luciferase by binding to FR. If the GFP-dnE1 construct retains dnE1 function, co-expressing EBNA1 and GFP-dnE1 should reduce reporter activity. Luciferase activity was increased significantly upon EBNA1 expression by approximately 5.3-fold, consistent with previous findings (Fig. 1B, $P < 0.05$, two-tailed Student's t-test).[17] When GFP-dnE1 was co-expressed, the luciferase activity was decreased. The decrease in luciferase activity was proportional to the increase in GFP-dnE1 expression vector (Fig. 1B, maximum reduction: 22.3%, $P < 0.05$, two-tailed Student's t-test). This effect was not observed with GFP alone. In addition, CMV promoter-driven luciferase expression was unaffected by EBNA1, GFP-dnE1, and GFP, suggesting that the reduction in luciferase activity with GFP-dnE1 in the EBNA1/FR-tk-luciferase system is specific. These data indicate that GFP-dnE1 functions as an inhibitor of EBNA1.

Establishment of B cells constitutively expressing GFP-dnE1. To investigate the potential effect of GFP-dnE1 on EBV infection in B cells, we established BALL-1 and BJAB cells, which constitutively express GFP-dnE1, using an MLV vector. GFP was used as a control throughout this study. The distribution of GFP-dnE1 was examined by confocal microscopy, which revealed an even distribution of GFP throughout the cell. In contrast, the majority of GFP-dnE1was localized to the nucleus due to the presence of the NLS (Fig. 2A). Similar observations were made in BJAB and 293T cells (data not shown). We sorted the GFP- or GFP-dnE-expressing cells using a FACS sorter. To test the dose-dependent effect, we collected BALL-1 cell populations bearing high or low levels of GFP fluorescence, denoted as Hi and Lo, respectively. The expression of GFP and GFP-dnE1 was verified by Western blotting, which confirmed that GFP and GFP-dnE1 Hi cells had higher intensity signals than the GFP and GFP-dnE1 Lo cells (Fig. 2B). The rate of cell proliferation and the morphology of GFP-dnE1 cells were indistinguishable from those of GFP cells (Fig. 2A and data not shown).

Effect of GFP-dnE1 on the nuclear translocation of EBV DNA during the acute phase of EBV infection. To assess whether GFP-dnE1 could restrict the nuclear targeting of the EBV
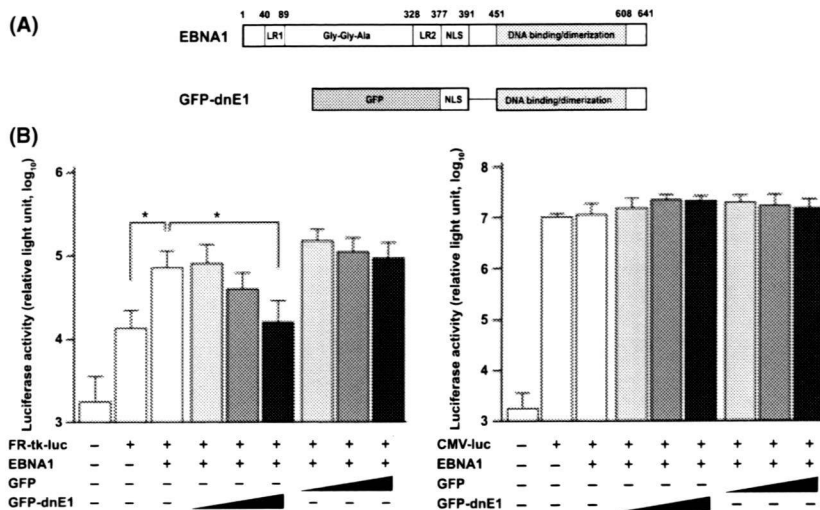
Fig. 1. Construction and functional characterization of a dominant-negative EBNA1 mutant (dnE1) fused to green fluorescent protein (GFP). (A) Structure of the EBNA1 protein and dnE1 used in this study. The linking regions (LR1 and LR2), the Gly-Gly-Ala repeat, the nuclear localization signal (NLS), and the DNA binding and dimerization domain are shown. GFP-dnE1 encodes the NLS and DNA binding and dimerization domain of EBNA1 fused to the C-terminus of GFP. (B) Repression of EBNA1-dependent transcriptional activation by GFP-dnE1. We transfected 293T cells in 48-well plates with 200 ng of FR-tk-luc or CMV-luc reporter, and 500 ng of EBNA1 expression vector, along with increasing amounts of GFP or GFP-dnE1 expression vector (20, 100, and 500 ng, respectively). *$P < 0.05$, two-tailed Student's t-test.
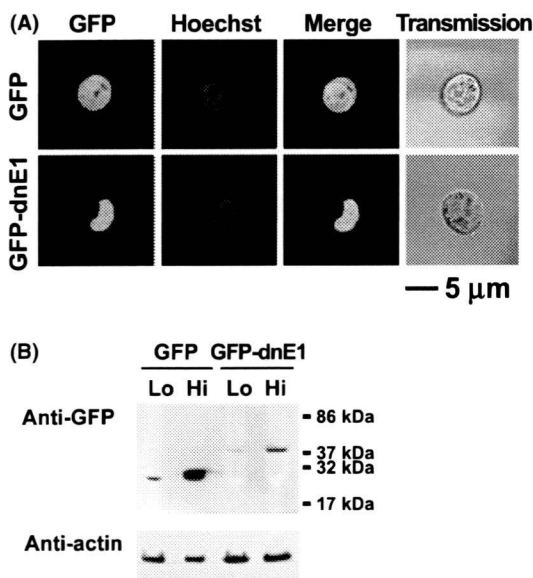

Fig. 2. Verification of stable green fluorescent protein (GFP)-dominant-negative EBNA1 (dnE1) expression in BALL-1 cells. (A) Distribution of GFP and GFP-dnE1 in BALL-1 cells was examined by confocal microscopy. Cells were imaged unfixed using a confocal microscope META 510 (Carl Zeiss, Tokyo, Japan). The green signal represents GFP fluorescence, and blue represents the Hoechst-stained nucleus. The bar represents 5 μm; magnification, ×630. (B) GFP or GFP-dnE1 expression in stably transduced BALL-1 cells was examined by Western blot analysis using an anti-GFP antibody. Protein lysates from 5×10^5 cells were loaded for each sample, except GFP Hi cells (5×10^4). The molecular weight marker is shown on the right.

genome after infection, we measured the amount of EBV DNA recovered from cells immediately after infection (representing the amount of EBV attached to cells) and the amount of EBV DNA that had migrated into the nucleus at 1 day post-infection. We isolated the nuclear fraction to exclude EBV DNA that

failed to enter the nucleus. The number of EBV DNA molecules per cell was estimated by real-time PCR, which targeted the BamHI W repeat, in 10 ng of genomic DNA. We estimated the number of EBV DNA per cell given that a single cell contains approximately 10 pg of genomic DNA, and an EBV DNA has 10 copies of BamHI W repeats on average. The nuclear targeting efficiencies of EBV DNA were as follows: BALL-1 GFP cells, 43.3–108.6%; GFP-dnE1 cells, 46.9–65.6%; BJAB GFP cells, 37.4%; GFP-dnE1 cells, 35.0% (Table 1). These data suggested that the effect of GFP-dnE1 on the nuclear targeting of EBV DNA should be assessed more sensitively in BALL-1 and BJAB cell systems than in primary B cells because the nuclear targeting efficiency of EBV DNA in primary B cells is extremely inefficient (~1.1%).[13] In our experimental systems, the nuclear targeting efficiencies of EBV DNA in GFP-dnE1-expressing cells were similar to those in GFP-expressing cells. In addition, the dose-dependency of GFP-dnE1 was not observed in BALL-1 cells (Table 1). These data suggest that the nuclear targeting efficiency of EBV DNA was not restricted by the presence of GFP-dnE1 in B cells upon EBV infection.

Effect of GFP-dnE1 on the rate of loss of EBV DNA during the acute phase of EBV infection. To examine the effect of GFP-dnE1 on the rate of loss (ROL) of EBV DNA during the acute phase of viral infection, we monitored the EBV DNA copy number from day 2 to day 5 or day 6 post-infection, by real-time PCR, which detects the viral genome in both linear and circular configurations (Table 1). The ROL was estimated as the percentage reduction of EBV DNA per cell generation, considering that the cell doubling time is 24 h, and the kinetics of viral genome loss follows an exponential decay. The ROL in GFP-dnE1-expressing cells (19.2–85.9% per cell generation) was similar to GFP-expressing cells (20.5–79.4% per cell generation) in both BALL-1 and BJAB cells. In addition, there was no detectable dose-dependent effect of GFP-dnE1 in BALL-1 cells (Table 1 and Fig. 3). The averages ± SEs of ROL in GFP- and GFP-dnE1-expressing cells from six independent measurements in BALL-1 cells were 37.7 ± 10.7% and 25.7 ± 6.5% per cell generation, respectively (data not shown), which was substantially higher than the rate of loss of an established oriP replicon (2–4%).[10,11] These results reflect the precipitous loss of oriP plas-

Kariya *et al.*

Table 1. The kinetics of EBV DNA in the acute phase of EBV infection

Cell	Copy number of EBV DNA per cell at the indicated day†				Nuclear transport (%‡)	Rate of loss of EBV DNA (% per cell generation§)
Expt 1						
BALL-1	Day 0	Day 1	Day 2	Day 5		
GFP Hi	20.38	11.92	3.57	0.01¶	58.5	85.9
GFP Lo	17.26	11.68	3.21	0.56	67.7	44.1
GFP-dnE1 Hi	23.02	10.79	3.30	0.30	46.9	54.9
GFP-dnE1 Lo	18.83	12.36	1.46	0.53	65.6	28.7
BJAB	Day 0	Day 1	Day 2	Day 5		
GFP	155.1	58.8	5.38	0.06	37.4	77.7
GFP-dnE1	64.6	37.4	5.69	0.05	58.0	79.4
Expt 2						
BALL-1	Day 0	Day 1	Day 2	Day 6		
GFP Hi	16.33	17.73	11.10	4.74	108.6	19.2
GFP Lo	17.35	7.51	8.75	1.13	43.3	40.1
GFP-dnE1 Hi	18.46	8.71	8.95	3.38	47.2	21.6
GFP-dnE1 Lo	14.14	7.05	6.97	2.79	49.9	20.5

†Nuclear DNA was used for day 1 data. ‡Estimated from day 0 and day 1 data. §Estimated from day 2 and day 5 or day 6 data with the exponential decay. ¶Below the limit of detection. dnE1, dominant-negative EBNA1; EBV, Epstein–Barr virus; GFP, green fluorescent protein.
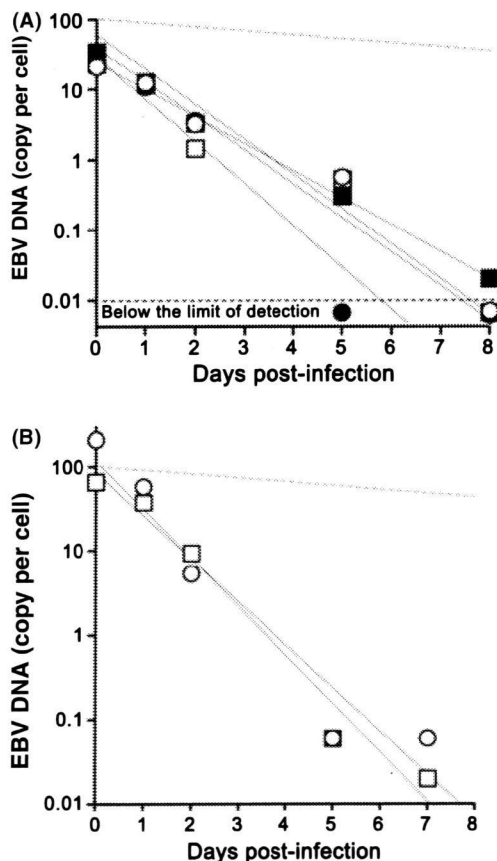

Fig. 3. Kinetics of Epstein–Barr virus (EBV) DNA loss during the acute phase of EBV infection. (A) Representative data from BALL-1 cells (Expt. 1 in Table 1) is shown. The filled squares, open squares, filled circles, and open circles represent GFP Hi, GFP Lo, GFP-dnE1 Hi, and GFP-dnE1 Lo, respectively. The limit of detection was below 0.01 (dashed line). The gray lines represent an approximation to the exponential decay. The dashed gray line represents the 4% rate of loss per cell generation. (B) Representative data from BJAB cells shown in Table 1. The circles and squares represent GFP and GFP-dnE1, respectively. Please see Table 1 for the detailed analysis.

mids (26–37%) in transiently transfected non-B cells.[12] The data suggest that GFP-dnE1 is unable to accelerate the ROL in the acute phase of EBV infection in B cells, presumably because the EBV genome is not established as an EBNA1-dependent stable licensed replicon. It should be noted that this is the first time that quantitative ROL data has been obtained by introducing the oriP replicon into B cells via EBV infection, which is an approach that does not confer any selective advantage on the infected cells.

Effect of GFP-dnE1 on efficiency of establishment of EBV latency. Cells infected with recombinant EBV$_3$ carrying the neomycin resistance gene, were seeded at 5×10^3 cells per well into a 96-well plate, and the efficiency of the establishment of EBV latency was assessed as the percentage of wells positive for the emergence of G418-resistant cells. G418-resistant cells appeared in BJAB, Daudi, parental BALL-1, and BALL-1 GFP cells at 56–100% efficiencies. In sharp contrast, G418-resistant cells were absent from GFP-dnE1-expressing BALL-1 cells (Table 2). These data clearly suggest that, although the ROL during the acute phase of EBV infection was not enhanced by GFP-dnE1, GFP-dnE1 was able to block the establishment of EBV latency completely during the subacute phase of EBV infection.

Effect of GFP-dnE1 on EBV-encoded latent gene expression. EBV gene expression was tested at 2 days post-infection by quantitative RT-PCR. We focused on the C/Wp activity because it expresses key viral transactivators including EBNA1, -2, -3s, and -LP to boost viral transforming gene expression. We detected C/Wp-driven transcripts in GFP Hi BALL-1 cells as expected. Conversely, C/Wp-driven transcripts were undetectable in GFP-dnE1 Hi and Lo BALL-1 cells, although these cells retained similar EBV DNA levels to GFP-expressing cells (Fig. 4 and Table 3). The Cp-driven transcript was under the limit of detection by RT-PCR, suggesting that the Wp is predominantly activated at the early phase of EBV infection consistent with previous findings.[7] Inhibition of viral gene transcription was not observed in the RNA polymerase III-driven transcript EBER1,[25] and cyclophilin A mRNA levels were similar between GFP- and GFP-dnE1-expressing cells (Fig. 4 and Table 3). This indicates that the effect of GFP-dnE1 on C/Wp activity is specific, and uncovers an active role of EBNA1 in supporting transactiva-

4

Table 2. The establishment efficiency of EBV latency

Cell	Emergence of G418-resistant cells†	
BJAB	100%	(6/6)
Daudi	100%	(10/10)
BALL-1		
Parental	56%	(5/9)
GFP Hi	67%	(2/3)
GFP-dnE1 Hi	0%	(0/6)
GFP-dnE1 Lo	0%	(0/6)

†Percentage of wells positive for G418-resistant cells over the number of tested wells from 96-well plates indicated in the bracket. Shown are the sum of two independent experiments. dnE1, dominant-negative EBNA1; EBV, Epstein–Barr virus; GFP, green fluorescent protein.
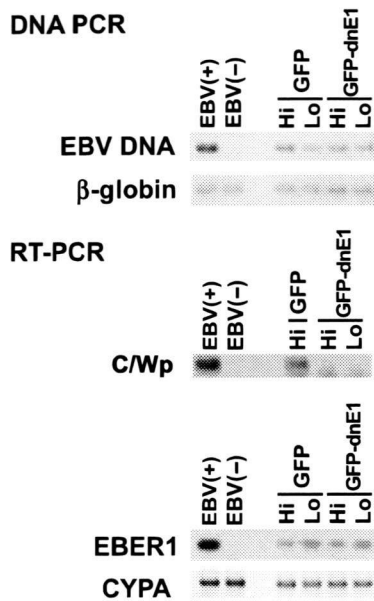

Fig. 4. PCR-based analysis of Epstein–Barr virus (EBV) gene expression. The effect of green fluorescent protein (GFP)-dominant-negative EBNA1 (dnE1) on the loss of EBV DNA (DNA PCR, upper panels) and transcription of the C/W promoter-driven transcript (C/Wp), EBER1, and cyclophilin A (CYPA; RT-PCR, lower panels) in BALL-1 cells at 2 days post-infection were examined. EBV-transformed B-lymphoblastoid cell line (B-LCL) and BJAB cells, denoted as EBV(+) and EBV(−), were used as positive and negative controls for viral DNA and RNA shown, respectively. β-Globin and CYPA were used as controls.

Table 3. Quantification of EBV transcripts in BALL-1 cells by real-time PCR at 2 days post-infection

BALL-1 cells		W1/2 exon (copies†)	EBER1 (copies‡)	CYPA (copies‡)
GFP	Hi	2.2	2.8×10^2	1.4×10^6
	Lo	NT§	0.8×10^2	1.0×10^6
GFP-dnE1	Hi	BLD¶	3.3×10^2	1.3×10^6
	Lo	BLD¶	1.2×10^2	1.5×10^6

†Copies per 13–14 ng total cellular RNA. ‡Copies per 200 ng total cellular RNA. §Not tested. ¶Below the limit of detection. CYPA, cyclophilin A; dnE1, dominant-negative EBNA1; EBV, Epstein–Barr virus; GFP, green fluorescent protein.

tion from C/Wp. Taken together, these results show that inhibition of EBNA1 functions strongly restricts EBV-encoded transforming gene expression and, although there is no detectable effect on the ROL of EBV DNA at the acute phase of viral infection, it blocks the establishment of EBV latency during the subacute phase.

Discussion

This is the first report describing the effect of EBNA1 inhibition from the onset of EBV infection in B cells. Unexpectedly, the dnE1 was unable to accelerate the ROL during the acute phase of EBV infection since dnE1 enhanced the loss of the oriP plasmid in the transient transfection assays.[10,11] In the subacute phase of EBV infection, the establishment of EBV latency was potently blocked by dnE1. In addition, we observed a strong repressive effect of dnE1 on the EBNA1-dependent enhancement of viral gene transcription from C/Wp during the early phase of EBV infection, similar to the transient transfection assays.[17] These data suggest that viral oncogene expression depends heavily on EBNA1 during the acute phase of viral infection, and that EBNA1 contributes little to EBV genome maintenance during this period. The results emphasize that an EBNA1 inhibitor should serve as an attenuator of viral oncogene expression since activation of C/Wp is the 'root' event of the positive feedback loop involved in the transactivation of viral transforming gene expression. In this regard, the EBNA1 inhibition approach could be superior to LMP-1 or EBNA2 inhibition.

If EBNA1 binding to oriP is essential for both the enhancement of viral gene transcription and for genome maintenance, what mechanism prevents dnE1 from affecting the ROL during the acute phase of EBV infection? It is likely that maintenance of the oriP replicon immediately after its introduction into cells is less efficient than in cells harboring an 'established' oriP replicon as an autonomously replicating plasmid. The ROL of an established oriP replicon is 2–4% per cell generation.[10,11] In contrast, our data from the EBV/B cell-based assay gave an average ROL of 26–38% during the week post-infection (acute phase of EBV infection). In agreement with our findings, it is reported that a transiently transduced oriP replicon is lost from cells at 26–37% per cell generation 1–2 weeks post-plasmid transduction.[12] These data indicate that maintenance of the oriP replicon is largely EBNA1-independent immediately after its introduction into cells, regardless of whether the route of introduction is by transfection or EBV infection. In other words, the establishment of EBV latency should be a rare epigenetic event. The data also suggest that the artificial minichromosome approach may be relevant in understanding EBV genome behavior.[12]

Our study suggests that gene therapy using GFP-dnE1 is an attractive approach, not only for therapeutics, but also for prophylactic interventions of EBV-associated malignancies. For example, in peripheral blood stem cell transplantation (PBSCT), GFP-dnE1 transduction into CD34+ cells should protect the differentiated B cells from EBV infection, thus preventing the genesis of EBV-associated B cell lymphomas. We will attempt to prove this hypothesis using a small animal model in future studies.[26] Additionally, EBNA1 is a potential molecular target for developing a small molecular-weight EBV inhibitor as mentioned previously.[14,15] The advantages of EBNA1-inhibitor development are that the biological assay system is already established and the X-ray crystal structure of the DNA-bound EBNA1 DNA binding and dimerization domain is known, which means that computer-aided drug design technology can be immediately applied. Although EBV is associated with various malignancies, preventive and therapeutic measures against EBV infection have not been developed. We believe that an anti-EBV agent, such as an EBNA1 inhibitor, would have an enormous impact in the medical field due to the substantial number of patients with EBV-associated malignancies.

Kariya et al.

Acknowledgments

Disclosure Statement

The authors have no conflict of interest.

References

1 Thompson MP, Kurzrock R. Epstein–Barr virus and cancer. *Clin Cancer Res* 2004; **10**: 803–21.
2 Rickinson AB, Kieff E. Epstin–Barr virus. In: Knipe DM, Howley PM, eds. *Fields Virology*, 5th edn, vol. 2. Philadelphia: Lippincott Williams & Wilkins, 2007; 2655–700.
3 Klein E, Kis LL, Klein G. Epstein–Barr virus infection in humans: from harmless to life endangering virus-lymphocyte interactions. *Oncogene* 2007; **26**: 1297–305.
4 Snow AL, Martinez OM. Epstein–Barr virus: evasive maneuvers in the development of PTLD. *Am J Transplant* 2007; **7**: 271–7.
5 Besson C, Goubar A, Gabarre J *et al.* Changes in AIDS-related lymphoma since the era of highly active antiretroviral therapy. *Blood* 2001; **98**: 2339–44.
6 Carbone A, Cesarman E, Spina M, Gloghini A, Schulz TF. HIV-associated lymphomas and gamma-herpesviruses. *Blood* 2009; **113**: 1213–24.
7 Kieff E, Rickinson AB. Epstin–Barr virus and its replication. In: Knipe DM, Howley PM, eds. *Fields Virology*, 5th edn, vol. 2. Philadelphia: Lippincott Williams & Wilkins, 2007; 2603–54.
8 Lindner SE, Sugden B. The plasmid replicon of Epstein–Barr virus: mechanistic insights into efficient, licensed, extrachromosomal replication in human cells. *Plasmid* 2007; **58**: 1–12.
9 Wang J, Sugden B. Origins of bidirectional replication of Epstein–Barr virus: models for understanding mammalian origins of DNA synthesis. *J Cell Biochem* 2005; **94**: 247–56.
10 Kirchmaier AL, Sugden B. Plasmid maintenance of derivatives of oriP of Epstein–Barr virus. *J Virol* 1995; **69**: 1280–3.
11 Sugden B, Warren N. Plasmid origin of replication of Epstein–Barr virus, oriP, does not limit replication in cis. *Mol Biol Med* 1988; **5**: 85–94.
12 Leight ER, Sugden B. Establishment of an oriP replicon is dependent upon an infrequent, epigenetic event. *Mol Cell Biol* 2001; **21**: 4149–61.
13 Hurley EA, Thorley-Lawson DA. B cell activation and the establishment of Epstein–Barr virus latency. *J Exp Med* 1988; **168**: 2059–75.
14 Altmann M, Pich D, Ruiss R, Wang J, Sugden B, Hammerschmidt W. Transcriptional activation by EBV nuclear antigen 1 is essential for the expression of EBV's transforming genes. *Proc Natl Acad Sci U S A* 2006; **103**: 14188–93.
15 Kennedy G, Komano J, Sugden B. Epstein–Barr virus provides a survival factor to Burkitt's lymphomas. *Proc Natl Acad Sci U S A* 2003; **100**: 14269–74.
16 Nasimuzzaman M, Kuroda M, Dohno S *et al.* Eradication of Epstein–Barr virus episome and associated inhibition of infected tumor cell growth by adenovirus vector-mediated transduction of dominant-negative EBNA1. *Mol Ther* 2005; **11**: 578–90.
17 Kirchmaier AL, Sugden B. Dominant-negative inhibitors of EBNA-1 of Epstein–Barr virus. *J Virol* 1997; **71**: 1766–75.
18 Komano J, Miyauchi K, Matsuda Z, Yamamoto N. Inhibiting the Arp2/3 complex limits infection of both intracellular mature vaccinia virus and primate lentiviruses. *Mol Biol Cell* 2004; **15**: 5197–207.
19 Aiyar A, Sugden B. Fusions between Epstein–Barr viral nuclear antigen-1 of Epstein–Barr virus and the large T-antigen of simian virus 40 replicate their cognate origins. *J Biol Chem* 1998; **273**: 33073–81.
20 Middleton T, Sugden B. EBNA1 can link the enhancer element to the initiator element of the Epstein–Barr virus plasmid origin of DNA replication. *J Virol* 1992; **66**: 489–95.
21 Urano E, Kariya Y, Futahashi Y *et al.* Identification of the P-TEFb complex-interacting domain of Brd4 as an inhibitor of HIV-1 replication by functional cDNA library screening in MT-4 cells. *FEBS Lett* 2008; **582**: 4053–8.
22 Shimizu S, Urano E, Futahashi Y *et al.* Inhibiting lentiviral replication by HEXIM1, a cellular negative regulator of the CDK9/cyclin T complex. *AIDS* 2007; **21**: 575–82.
23 Kanda T, Yajima M, Ahsan N, Tanaka M, Takada K. Production of high-titer Epstein–Barr virus recombinants derived from Akata cells by using a bacterial artificial chromosome system. *J Virol* 2004; **78**: 7004–15.
24 Mackey D, Sugden B. The linking regions of EBNA1 are essential for its support of replication and transcription. *Mol Cell Biol* 1999; **19**: 3349–59.
25 Howe JG, Shu MD. Epstein–Barr virus small RNA (EBER) genes: unique transcription units that combine RNA polymerase II and III promoter elements. *Cell* 1989; **57**: 825–34.
26 Yajima M, Imadome K, Nakagawa A *et al.* A new humanized mouse model of Epstein–Barr virus infection that reproduces persistent infection, lymphoproliferative disorder, and cell-mediated and humoral immune responses. *J Infect Dis* 2008; **198**: 673–82.

Dys-Regulated Activation of a Src Tyroine Kinase Hck at the Golgi Disturbs *N*-Glycosylation of a Cytokine Receptor Fms

RANYA HASSAN,[1] SHINYA SUZU,[1] MASATERU HIYOSHI,[1] NAOKO TAKAHASHI-MAKISE,[1] TAKAMASA UENO,[2] TSUTOMU AGATSUMA,[3] HIROFUMI AKARI,[4] JUN KOMANO,[5] YUTAKA TAKEBE,[6] KAZUO MOTOYOSHI,[7] AND SEIJI OKADA[1]*

[1] Division of Hematopoiesis, Center for AIDS Research, Kumamoto University, Kumamoto, Kumamoto, Japan

[2] Viral Immunology, Center for AIDS Research, Kumamoto University, Kumamoto, Kumamoto, Japan

[3] Tokyo Research Laboratories, Kyowa Hakko Co., Ltd, Machida, Tokyo, Japan

[4] Laboratory of Disease Control, Tsukuba Primate Research Center, National Institute of Biomedical Innovation, Tsukuba, Ibaraki, Japan

[5] Laboratory of Virology and Pathogenesis, AIDS Research Center, National Institute of Infectious Diseases, Shinjuku, Tokyo, Japan

[6] Laboratory of Molecular Biology and Epidemiology, AIDS Research Center, National Institute of Infectious Diseases, Shinjuku, Tokyo, Japan

[7] Department of Internal Medicine, National Defense Medical College, Tokorozawa, Saitama, Japan

HIV-1 Nef accelerates the progression to AIDS by binding with and activating a Src kinase Hck, but underlying molecular basis is not understood. We revealed that Nef disturbed N-glycosylation/trafficking of a cytokine receptor Fms in an Hck-dependent manner, a possible trigger to worsen uncontrolled immune system. Here, we provide direct evidence that dys-regulated activation of Hck pre-localized to the Golgi apparatus causes this Fms maturation arrest. A striking change in Hck induced by Nef other than activation was its skewed localization to the Golgi due to predominant Golgi-localization of Nef. Studies with different Nef alleles and their mutants showed a clear correlation among higher Nef-Hck affinity, stronger Hck activation, severe Golgi-localization of Hck and severe Fms maturation arrest. Studies with a newly discovered Nef-Hck binding blocker 2c more clearly showed that skewed Golgi-localization of active Hck was indeed the cause of Fms maturation arrest. 2c blocked Nef-induced skewed Golgi-localization of an active form of Hck (Hck-P2A) and Fms maturation arrest by Nef/Hck-P2A, but showed no inhibition on Hck-P2A kinase activity. Our finding establishes an intriguing link between the pathogenesis of Nef and a newly emerging concept that the Golgi-localized Src kinases regulate the Golgi function.

Studies of HIV-1-infected patients and monkey models have demonstrated that Nef, a protein with no enzymatic activity encoded by the HIV-1 genome, is a critical determinant for the development of AIDS (Kestler et al., 1991; Deacon et al., 1995; Kirchhoff et al., 1995). Subsequent studies of HIV-1 transgenic (Tg) mice supported the idea. The expression of entire coding sequences of HIV-1 in CD4$^+$ T cells and macrophages caused an AIDS-like disease, which was abolished by Nef deletion (Hanna et al., 1998). This pathogenetic activity of Nef is supposed to be mediated by its binding with cellular proteins, and a well-defined partner of Nef is Hck (Saksela et al., 1995), a member of Src family tyrosine kinases expressed in macrophages. Other Src kinases (Lyn, Fyn, c-Src, and Lck) bind Nef but with lower affinities (Arold et al., 1998; Karkkainen et al., 2006; Trible et al., 2006). Importantly, the disruption of proline-rich PxxP motif of Nef, an essential motif to bind the Src homology 3 (SH3) domain of Hck, was sufficient to protect Tg mice from the AIDS-like disease, and wild-type Nef-induced disease progression was significantly delayed in Hck$^{-/-}$ mice (Hanna et al., 2001), indicating that high affinity Nef-Hck binding in macrophages is at least in part responsible for disease development and progression. However, unresolved issue is how Nef-Hck binding followed by activation of Hck (Moarefi et al., 1997;

Lerner and Smithgall, 2002) satisfactorily account for disease development and progression.

An important clue to the issue is that Nef predominantly localized to the Golgi apparatus (Greenberg et al., 1998; Drakesmith et al., 2005; Haller et al., 2007) and that Nef not only activated Hck but also induced skewed localization of Hck to the Golgi (Hung et al., 2007). The Golgi functions as a sorting hub and location of glycosylation for proteins, and several lines of evidence have revealed that Src kinases, shown to be involved in a wide array of intracellular signaling (reviewed in

Lowell, 2004), also play a role in the regulation of the Golgi structure/function. First, a fraction of Src kinases, including Hck, is physiologically found at the Golgi (David-Pfeuty and Nouvian-Dooghe, 1990; Kaplan et al., 1992; Ley et al., 1994; Bijlmakers et al., 1997; van't Hof and Resh, 1997; Carreno et al., 2000; Kasahara et al., 2004). Second, fibroblasts lacking three ubiquitous Src kinases (c-Src/Yes/Fyn) exhibited an aberrant Golgi structure composed of collapsed stacks and bloated cisternae (Bard et al., 2003). Third, an increased protein load entering the cis-Golgi from the endoplasmic reticulum activated the Golgi-localized Src kinases, which in turn regulated overall protein trafficking activity in the secretory pathway (Pulvirenti et al., 2008). Importantly, the study by Pulvirenti et al. indicates that coordinated regulation of activity of the Golgi-localized Src kinases is crucial to maintain the Golgi function, which raises an intriguing possibility that Nef affects protein trafficking process and thereby macrophage phenotype/function through skewed Golgi-localization of active Hck.

Indeed, we recently identified an aberrant function of Nef, which was possibly due to the skewed Golgi-localization of active Hck. We previously found that Nef inhibited the signal of M-CSF, a primary cytokine for macrophages (Suzu et al., 2005), which was a possible trigger to worsen uncontrolled immune systems in patients, as M-CSF is essential to maintain macrophages at an anti-inflammatory state (reviewed in Hamilton, 2008). Of interest was the role of Hck in this inhibitory activity of Nef (Hiyoshi et al., 2008). Nef reduced cell surface expression of M-CSF receptor Fms in myeloid cells and macrophages, which was the direct cause of the inhibitory activity of Nef on M-CSF signal. Importantly, such reduced cell surface expression of Fms was reproduced in transfected 293 cells, but only in co-expression with Hck. More importantly, the reduced cell surface expression was due to the accumulation of an immature under-N-glycosylated Fms at the Golgi (hereinafter called Fms maturation arrest). However, constitutive-active Hck alone failed to induce such Fms maturation arrest. These results indicate that Nef inhibits M-CSF signal by arresting Fms N-glycosylation and trafficking at the Golgi and that such Fms maturation arrest was not caused just because of Hck activation. Thus, a most likely cause of Nef-induced Fms maturation arrest was skewed Golgi-localization of active Hck. However, this intriguing hypothesis should be carefully and directly tested, because it will not only help to clarify molecular basis of this novel function of Nef through Hck, but also provide an excellent example of disease-associated failure of the Golgi function regulation by the Golgi-localized Src kinases.

In this study, we therefore sought to definitely conclude that skewed Golgi-localization of active Hck was indeed the direct cause of Fms maturation arrest by Nef. To this end, we employed two different approaches. First, we prepared various Nef proteins and compared their abilities to induce skewed Golgi-localization of Hck, Hck activation and Fms maturation arrest. Second and importantly, we discovered a small-molecule non-kinase inhibitor that effectively blocked Nef-Hck binding and performed mechanistic analyses with the newly discovered compound.

Materials and Methods
Expression plasmids

For the expression in HEK293 cells (Invitrogen, Carlsbad, CA), human Fms- and human p56Hck cDNA cloned into pCDNA3.1 vector (Invitrogen) were used (Suzu et al., 2005; Hiyoshi et al., 2008). The constitutive-active Hck P2A mutant (Hiyoshi et al., 2008) was also used in selected experiments. The expression plasmid for human Lyn cloned in pME-puro vector was provided by Y. Yamanashi (Tokyo Medical and Dental University, Tokyo, Japan) and used in the pull-down assay with GST-Nef fusion proteins (see

below). Nef cDNA derived from the NL43 or SF2 strain of HIV-1 was cloned into pRc/CMV-CD8 vector to express the extracellular/transmembrane regions of CD8-Nef fusion protein (Hiyoshi et al., 2008). NL43 Nef-M20A was prepared as described previously (Akari et al., 2000). NL43 Nef-AxxA and $-\Delta E$ mutant were provided by A. Adachi (University of Tokushima, Tokushima, Japan) and J.C. Guatelli (University of California, San Diego, CA), respectively. In this study, we prepared another NL43 Nef mutant (NL43 Nef-TR), by using QuikChange II Site-directed Mutagenesis Kits (Stratagene, La Jolla, CA). We also prepared Nef constructs expressing Nef-GFP fusion proteins (Ueno et al., 2008). For the expression of GST-Nef fusion proteins, fragments containing the entire coding sequences of the wild-type NL43 Nef, NL43 Nef-TR mutant, wild-type SF2 Nef, and SF2 Nef-AxxA mutant were subcloned into pGEX-6P-1 vector (GE Healthcare, Buckinghamshire, UK). SF2 Nef-AxxA mutant was prepared by using QuikChange II Site-directed Mutagenesis Kits (Stratagene). The nucleotide sequences of the coding region of all Nef constructs were verified by using BigDye Terminator v3.1 Cycle Sequencing Kit (Applied Biosystems, Foster City, CA) and ABI PRISM 3100 Genetic Analyzer (Applied Biosystems).

Chemicals

PP2 (Sigma, San Diego, CA) was used as the Src kinase inhibitor. UCS15A and its synthetic derivatives, 2b and 2c, were prepared as described (Oneyama et al., 2003). All these inhibitors were dissolved in dimethyl sulfoxide (DMSO; Wako, Osaka, Japan).

Western blotting

HEK293 cells were maintained with DME medium (Wako) supplemented with 10% fetal calf serum (FCS). The maturation of Fms proteins or the activation of Hck was analyzed by the transient expression assay with the cells followed by Western blotting as described previously (Suzu et al., 2005; Hiyoshi et al., 2008). In brief, cells grown on a 12-well tissue culture plate were transfected with plasmid for Fms (0.4 μg), Nef (0.8 μg), or Hck (0.4 μg) in the combinations indicated using LipofectAMINE2000 reagent (Invitrogen), unless otherwise stated. Total amounts of plasmids were normalized with the empty vectors. After 6 h, culture medium was replaced with complete medium and the transfected cells were cultured for an additional 42 h. In selected experiments, chemicals such as PP2 and 2c were added to the culture at the same time of changing medium. Total cell lysates were prepared essentially as described (Suzu et al., 2000). Primary antibodies used for Western blotting were as follows: anti-Fms (C-20; Santa Cruz Biotechnology, Santa Cruz, CA), anti-CD8 (H-160; Santa Cruz), anti-GFP (FL; Santa Cruz), anti-Hck (clone 18; Transduction Laboratories, Lexington, KY), anti-Hck phosphorylated at tyrosine 411 (Hck-pTyr[411]; Santa Cruz), anti-phosphotyrosine (PY99; Santa Cruz), and anti-ERK1/2 (K-23; Santa Cruz). The relative intensity of bands on scanned gel images was quantified using NIH Image software, and the Fms maturation arrest or Hck activation is also shown graphically on an arbitrary unit. The relative intensity of bands on Hck-pTyr[411] blots was quantified and the degree of Hck activation was expressed as a fold-increase relative to the control. For Fms maturation arrest, we calculated the percentage of immature under-N-glycosylated Fms of total Fms protein amount, and compared the percentages among samples.

Immunofluorescence

The signal of Nef-GFP was directly visualized with a BZ-8000 fluorescent microscope (Keyence, Osaka, Japan) equipped with Plan-Fluor ELWD 20x/0.45 objective lenses (Nikon, Tokyo, Japan) (Hiyoshi et al., 2008). To detect active Hck, cells were fixed in 2% paraformaldehyde, permeabilized with ethanol, and stained with goat anti-active Hck antibodies (Santa Cruz). Secondary antibodies were anti-goat IgG-AlexaFluo488 (Molecular Probes, Eugene, OR). Nuclei were stained with DAPI (Molecular Probes), and

fluorescent signals were visualized as above. Image processing was performed using BZ-analyzer (Keyence) and Adobe Photoshop Software (Adobe Systems, San Jose, CA).

GST pull-down

The control GST or GST-Nef fusion proteins (wild-type NL43 Nef, NL43 Nef-TR, wild-type SF2 Nef, and SF2 Nef-AxxA) cloned in pGEX-6P-1 vector was expressed in E. coli BL21 cells (GE Healthcare). Cells were grown in LB media containing 50 μg/ml ampicillin followed by induction with 1 μM IPTG. The expression-induced cells were harvested and lysed with BugBuster Protein Extraction Reagent containing 1 U/ml rLysozyme and 25 U/ml Benzonaze Nuclease (Novagen, Madison, WI). The cleared lysates were then incubated with GST-Bind Resin (Novagen). After extensive washing with GST Bind/Wash Buffer

(Novagen), the resin was incubated with the total cell lysates of HEK293 cells transfected with the expression plasmid for Hck or Lyn. In a selected experiment, 2c was added to the mixtures. After extensive re-washing, the resin was boiled with SDS–PAGE sample buffer and elutes were analyzed for the presence of Hck or Lyn by western blotting. Primary antibodies used were as follows (both from Transduction Laboratories): anti-Hck (clone 18) and anti-Lyn (clone 42). In a selected experiment, we also used GST proteins fused to the SH3 domain of Hck (Paliwal et al., 2007), which was provided by G. Swarup (Center for Cellular and Molecular Biology, Hyderabad, India).

Subcellular fractionation

The subcellular fractionation on sucrose gradients was performed exactly as reported (Matsuda et al., 2006). In brief, cells were
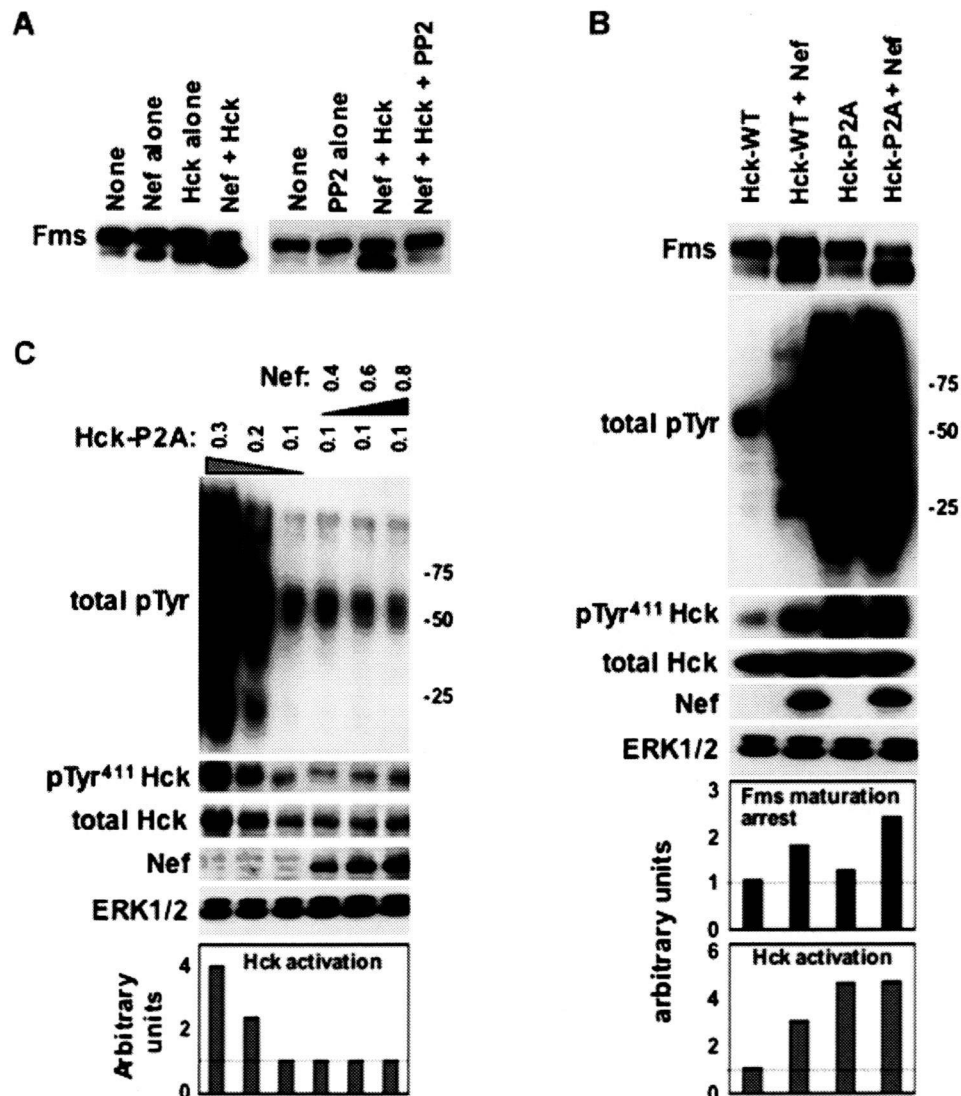

Fig. 1. Nef/Hck-induced Fms mturation arrest. A: HEK293 cells were transfected with Fms plamid alone (None) or co-transfected with the plasmids for NL43 Nef and/or wild-type Hck as indicated. In the right blot, PP2 was added to selected wells at a final concentration of 10 μM after the transfection. Total cell lysates were subjected to Fms Western blotting. B: Cells were transfected with Fms plasmid alone (None) or in combination with the plasmids for Nef (NL43) and Hck (WT or constitutive-active P2A), as indicated. These cells were then analyzed for the expression of Fms, tyrosine-phosphorylated proteins (total pTyr), active-Hck (pTyr^{411}Hck), total Hck, CD8-Nef (Nef), or ERK by Western blotting. The ERK blot is a loading control. The quantified Fms maturation arrest and Hck activation are shown in the bar graphs. C: Cells were transfected with varying amounts (μg) of Hck-P2A and NL43 Nef plasmids as indicated, and analyzed as in (B). The quantified Hck activation is shown in the bar graphs. [Color figure can be viewed in the online issue, which is available at www.interscience.wiley.com.]
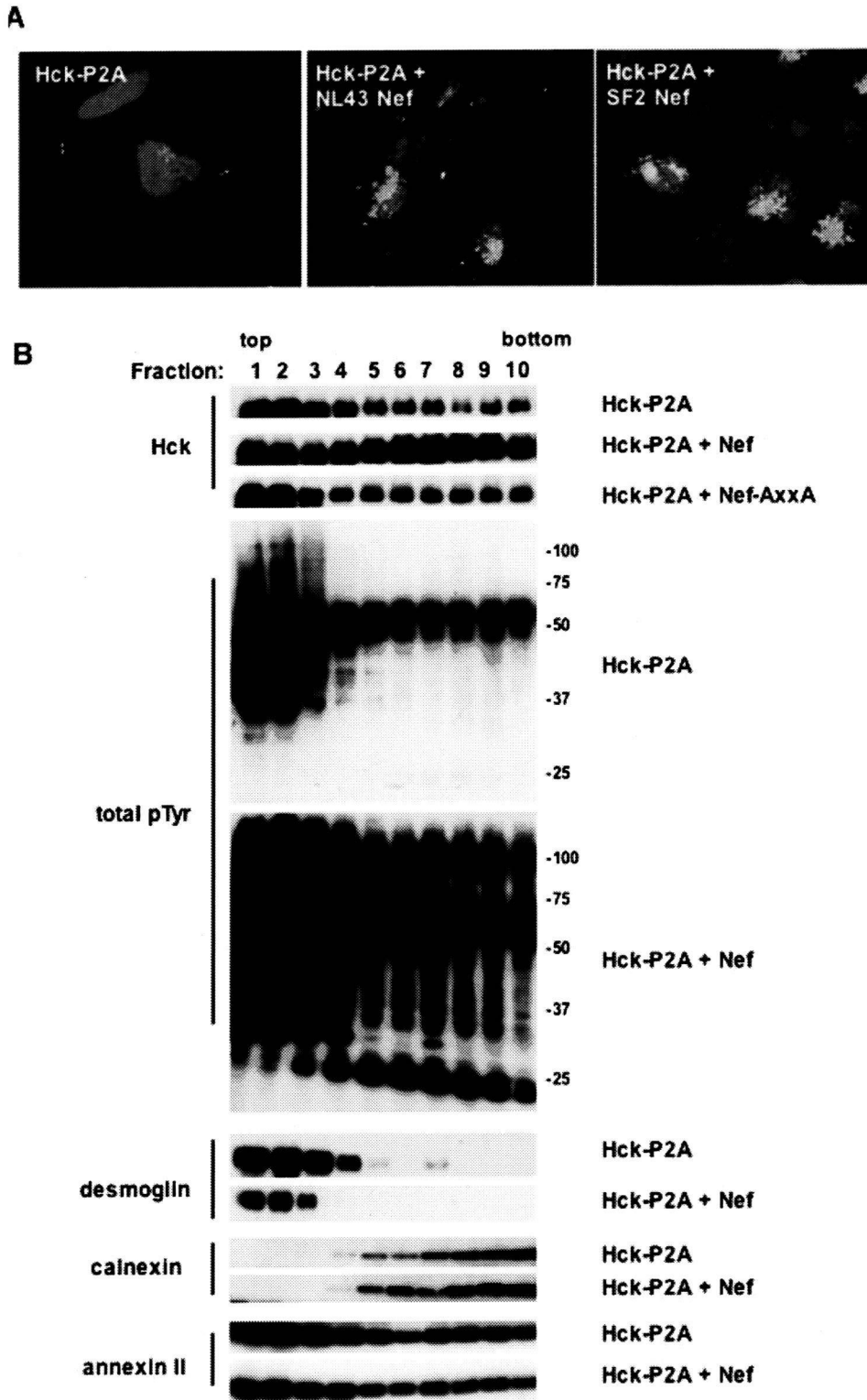
A

B

Fig. 2.   Skewed Golgi-localization of Hck by Nef. A: HEK293 cells were transfected with Hck-P2A plasmid alone, or co-transfected with NL43 Nef or SF2 Nef plasmid. Cells were stained with antibody specific for active Hck (green) and DAPI (blue). B: Cells were transfected with Hck-P2A alone, or co-transfected with NL43 Nef. Then, cells were subjected to subcellular fractionation on sucrose gradients and Western blotting with antibodies against Hck, phosphotyrosine (pTyr), desmoglein, calnexin, or annexin II. [Color figure can be viewed in the online issue, which is available at www.interscience.wiley.com.]